

Fig. 2-1 The setup of excimer laser crystallization

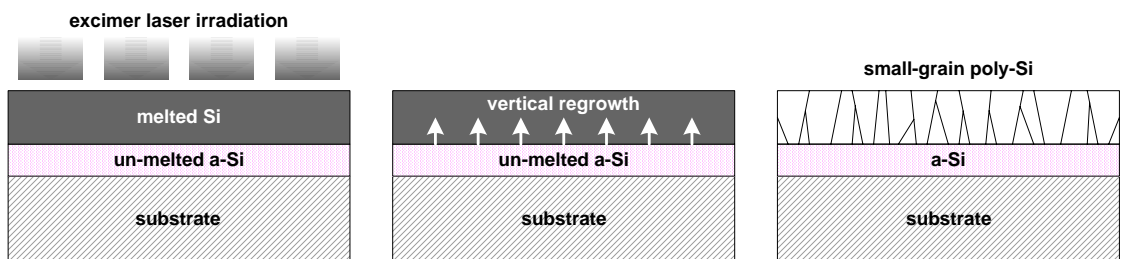


Fig. 2-2 Partially melted regime (low energy density regime)

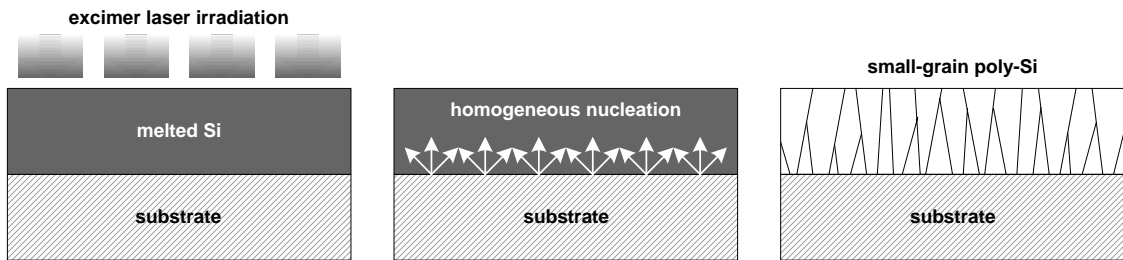


Fig. 2-3 Completely melted regime (high energy density regime)

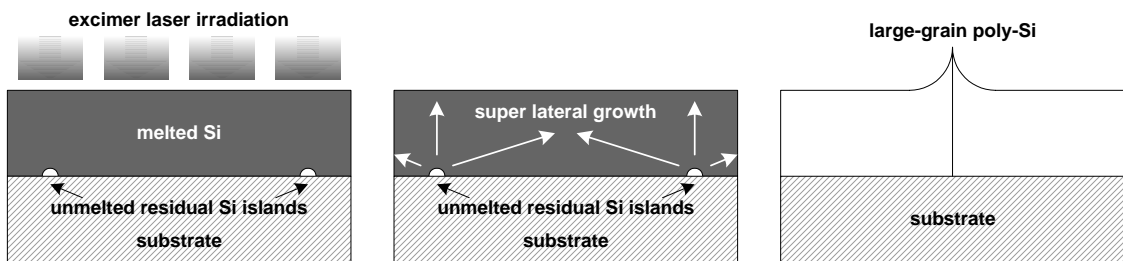


Fig. 2-4 Near-completely melted regime (super lateral growth regime)

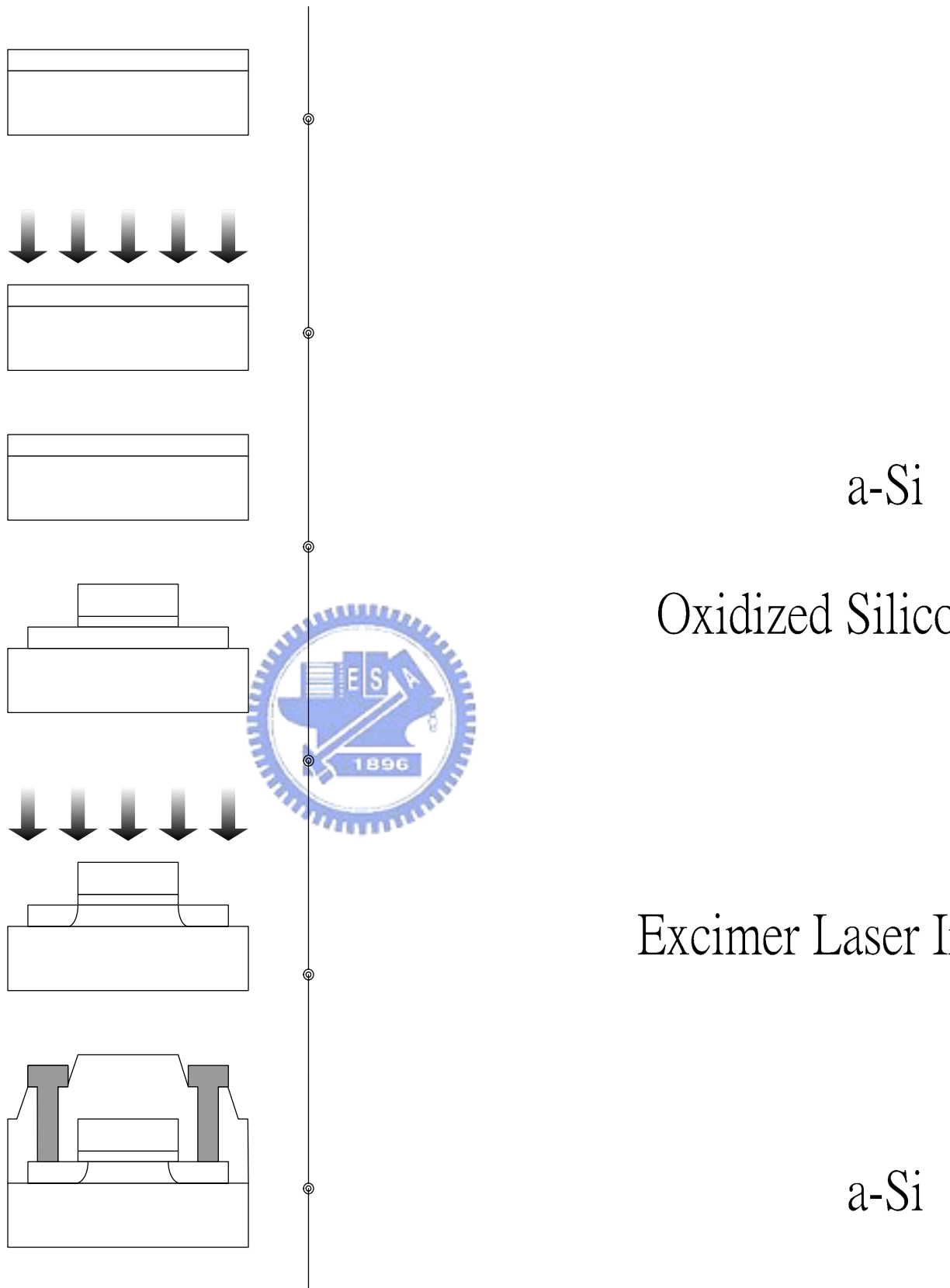


Fig. 2-5 Process flowchart of conventional ELC LTPS TFT

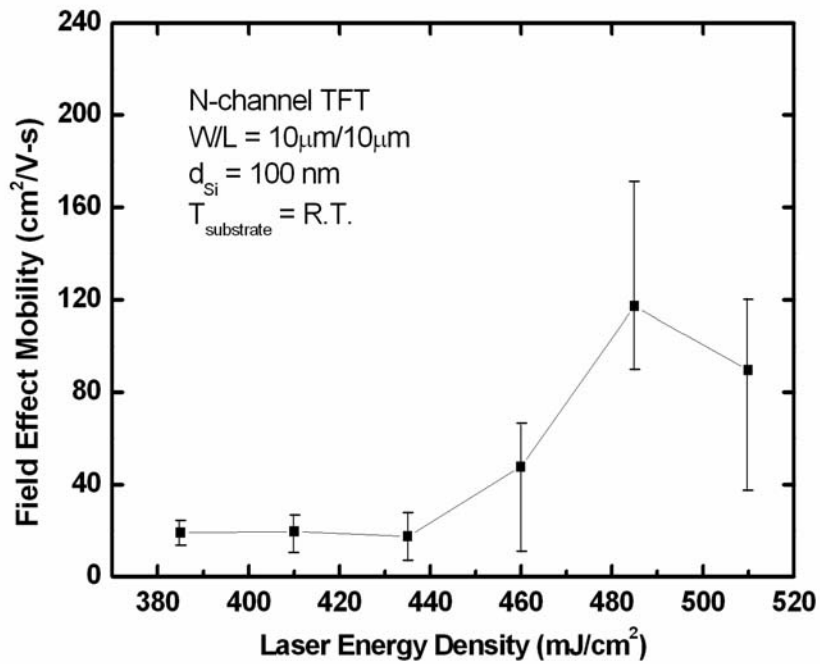


Fig. 2-6(a) Dependence of field effect mobility on laser energy density of 100nm conventional ELC LTPS TFTs for $W/L=10\mu\text{m}/10\mu\text{m}$ at RT.

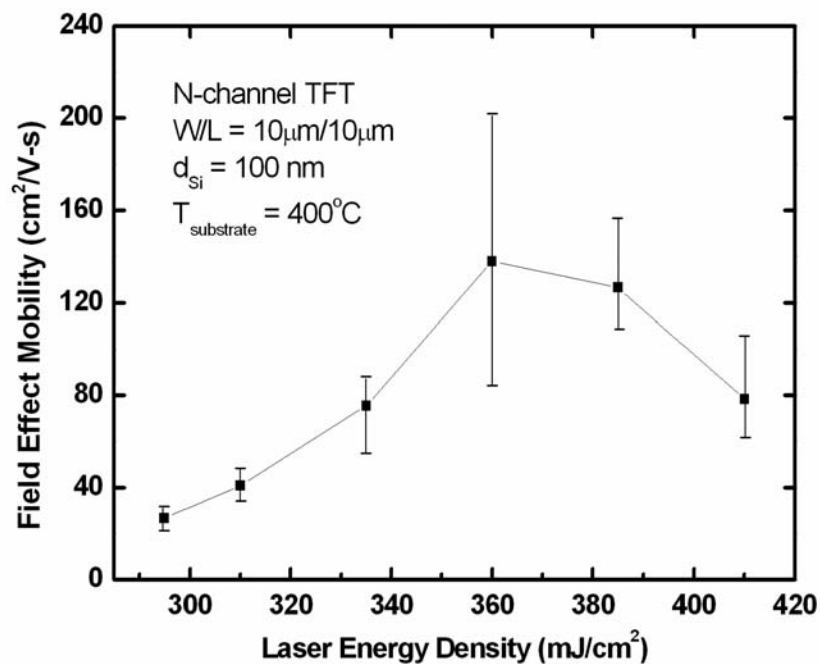


Fig. 2-6(b) Dependence of field effect mobility on laser energy density of 100nm conventional ELC LTPS TFTs for $W/L=10\mu\text{m}/10\mu\text{m}$ with substrate heating to 400°C

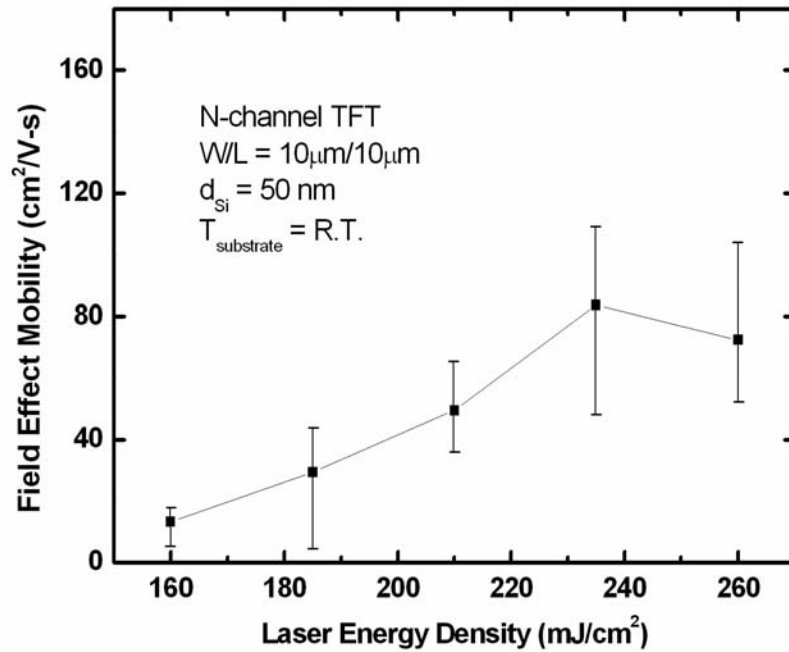


Fig. 2-7(a) Dependence of field effect mobility on laser energy density of 50nm conventional ELC LTPS TFTs for $W/L=10\mu\text{m}/10\mu\text{m}$ at RT.

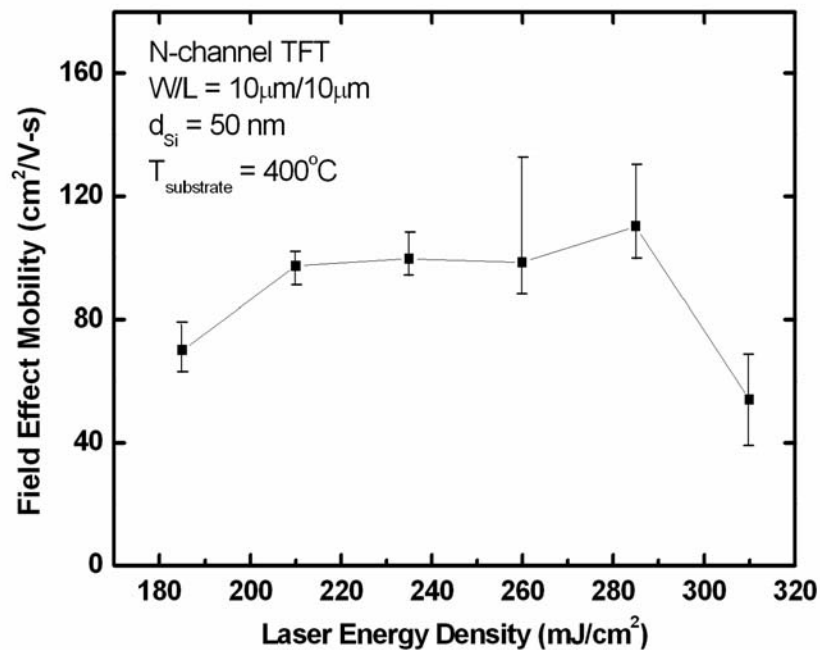


Fig. 2-7(b) Dependence of field effect mobility on laser energy density of 50nm conventional ELC LTPS TFTs for $W/L=10\mu\text{m}/10\mu\text{m}$ with substrate heating to 400°C

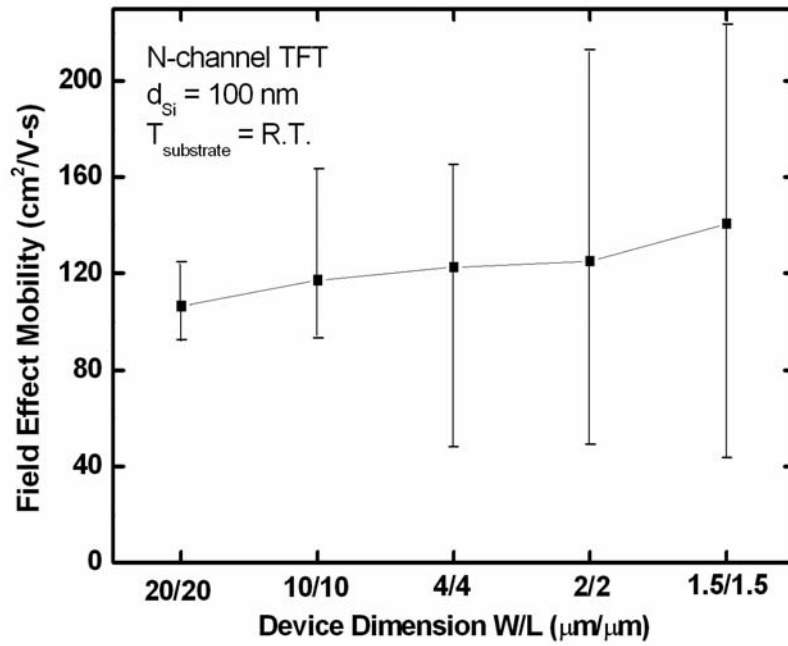


Fig. 2-8(a) Dependence of field effect mobility on device dimension of 100nm conventional ELC LTPS TFTs at RT

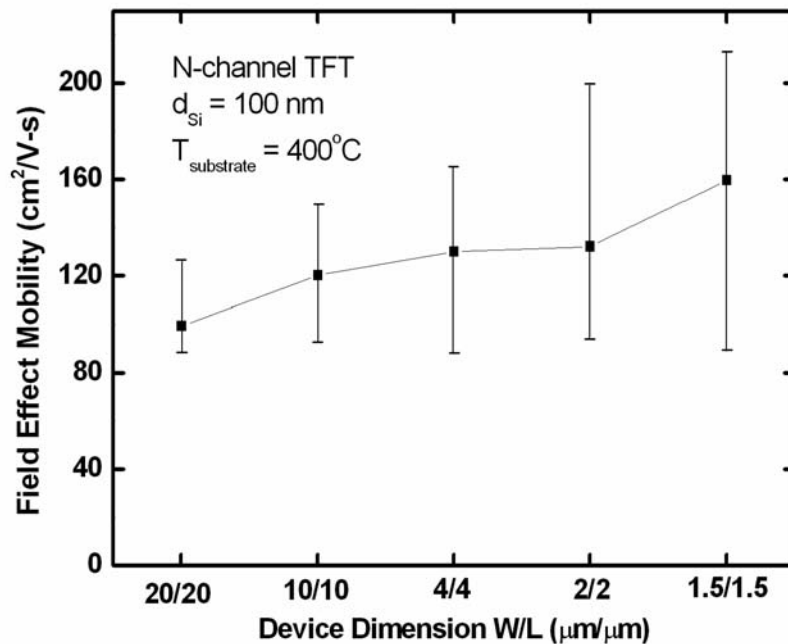


Fig. 2-8(b) Dependence of field effect mobility on device dimension of 100nm conventional ELC LTPS TFTs with substrate heating to 400°C

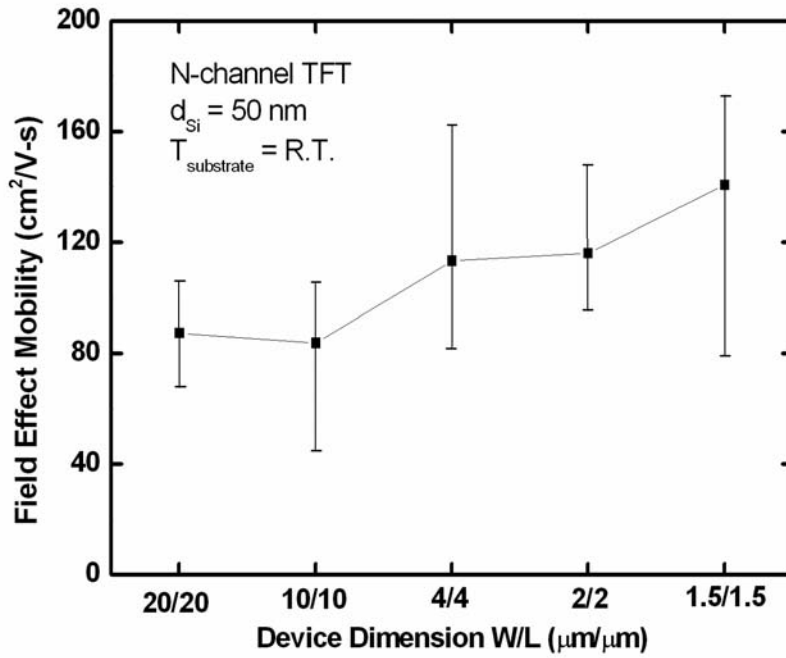


Fig. 2-9(a) Dependence of field effect mobility on device dimension of 50nm conventional ELC LTPS TFTs at RT

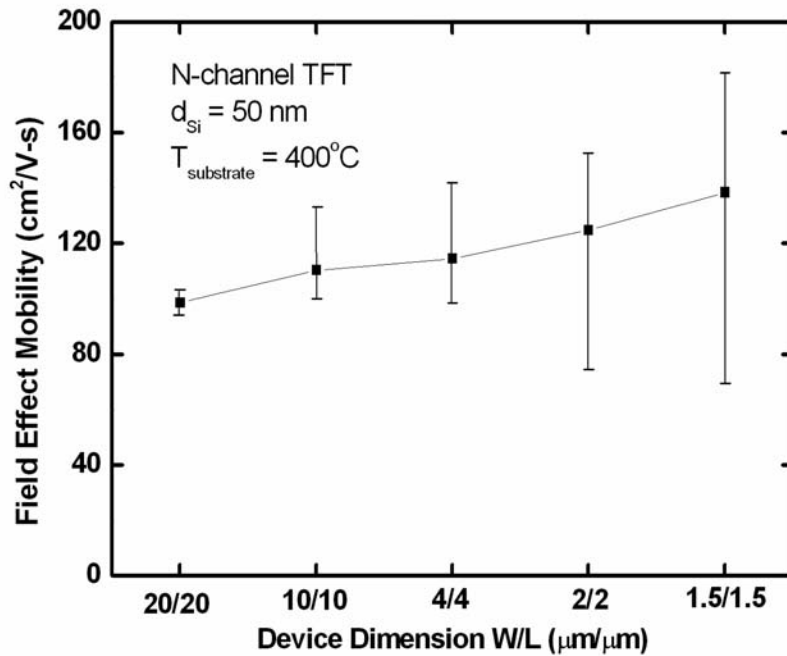


Fig. 2-9(b) Dependence of field effect mobility on device dimension of 50nm conventional ELC LTPS TFTs with substrate heating to 400°C

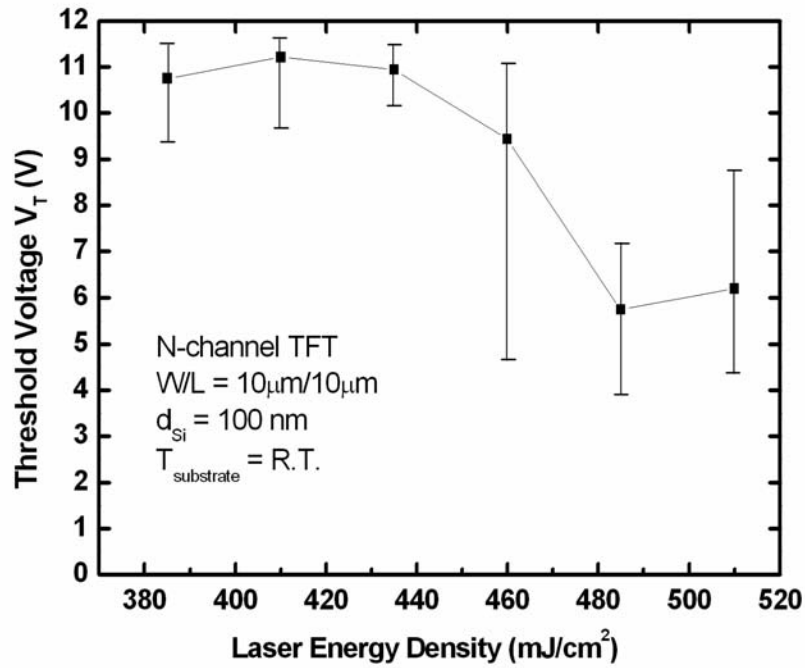


Fig. 2-10(a) Dependence of threshold voltage on laser energy density of 100nm conventional ELC LTPS TFTs for $W/L=10\mu\text{m}/10\mu\text{m}$ at RT.

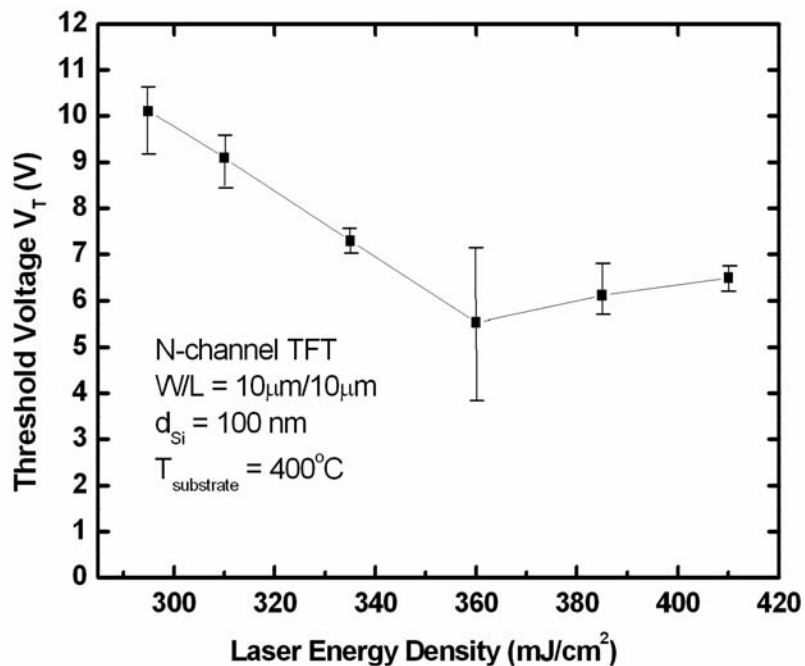


Fig. 2-10(b) Dependence of threshold voltage on laser energy density of 100nm conventional ELC LTPS TFTs for $W/L=10\mu\text{m}/10\mu\text{m}$ with substrate heating to 400°C

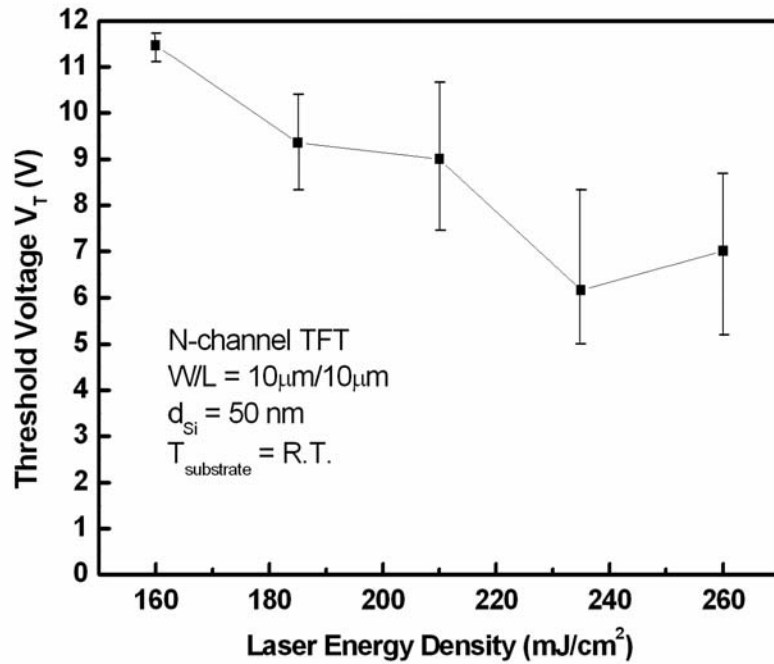


Fig. 2-11(a) Dependence of threshold voltage on laser energy density of 50nm conventional ELC LTPS TFTs for $W/L=10\mu\text{m}/10\mu\text{m}$ at RT.

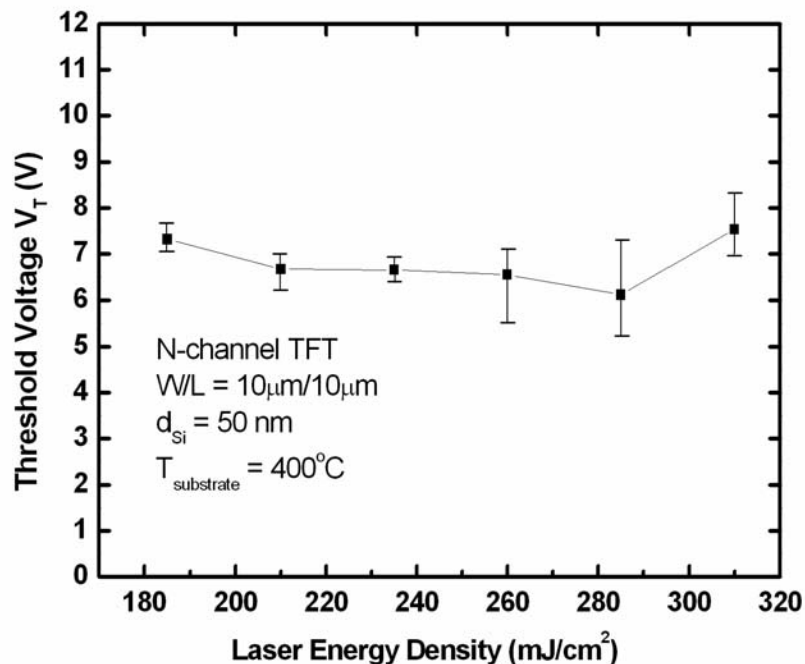


Fig. 2-11(b) Dependence of threshold voltage on laser energy density of 50nm conventional ELC LTPS TFTs for $W/L=10\mu\text{m}/10\mu\text{m}$ with substrate heating to 400°C

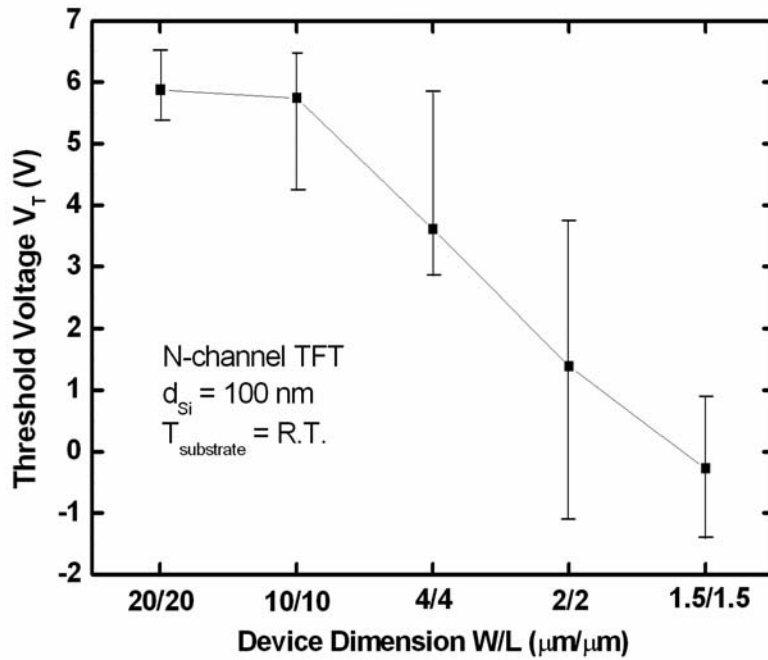


Fig. 2-12(a) Dependence of threshold voltage on device dimension of 100nm conventional ELC LTPS TFTs at RT

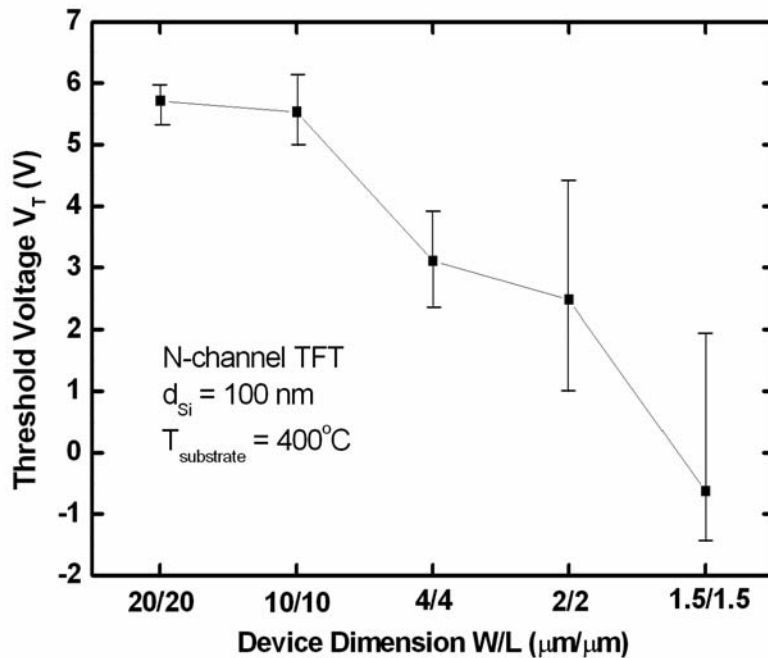


Fig. 2-12(b) Dependence of threshold voltage on device dimension of 100nm conventional ELC LTPS TFTs with substrate heating to 400°C

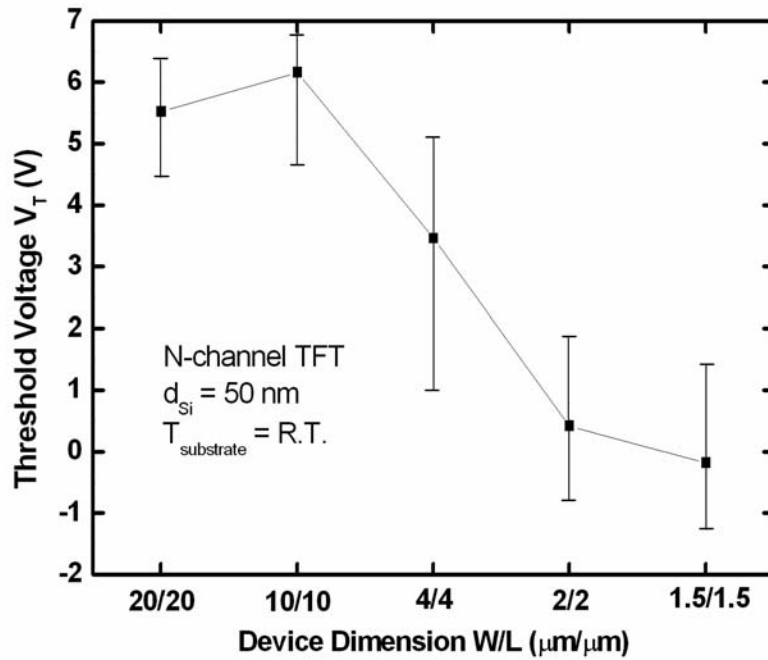


Fig. 2-13(a) Dependence of threshold voltage on device dimension of 50nm conventional ELC LTPS TFTs at RT

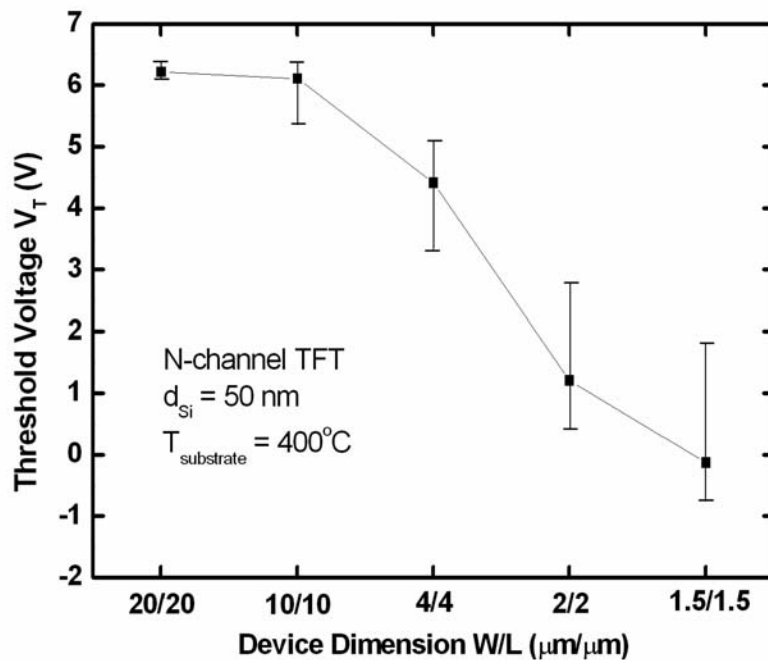


Fig. 2-13(b) Dependence of threshold voltage on device dimension of 50nm conventional ELC LTPS TFTs with substrate heating to 400°C

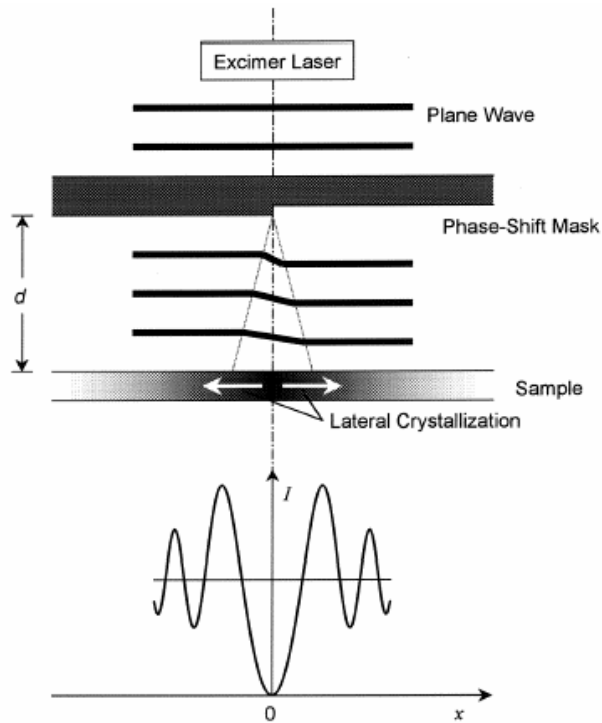


Fig. 2-14 The phase-modulated method

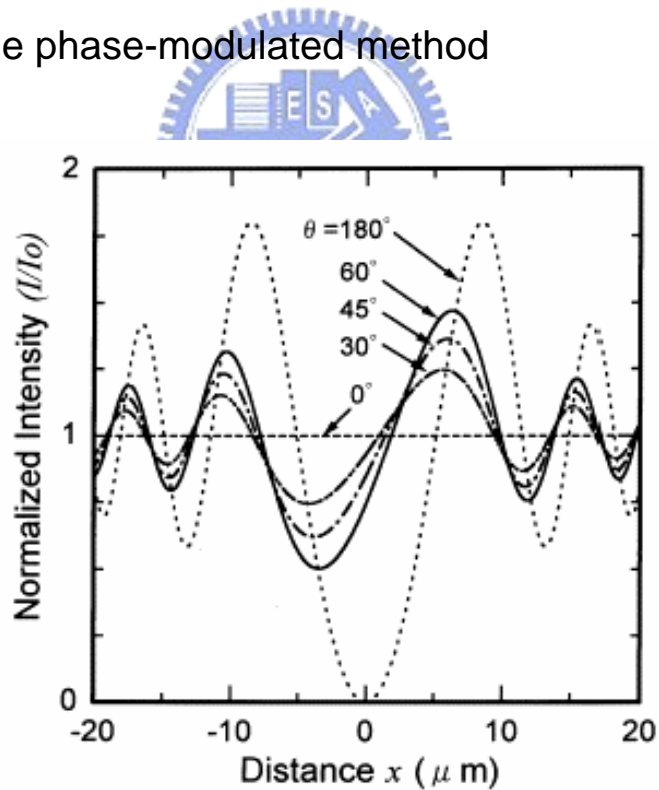


Fig. 2-15 The calculated intensity distribution as a function of the phase difference

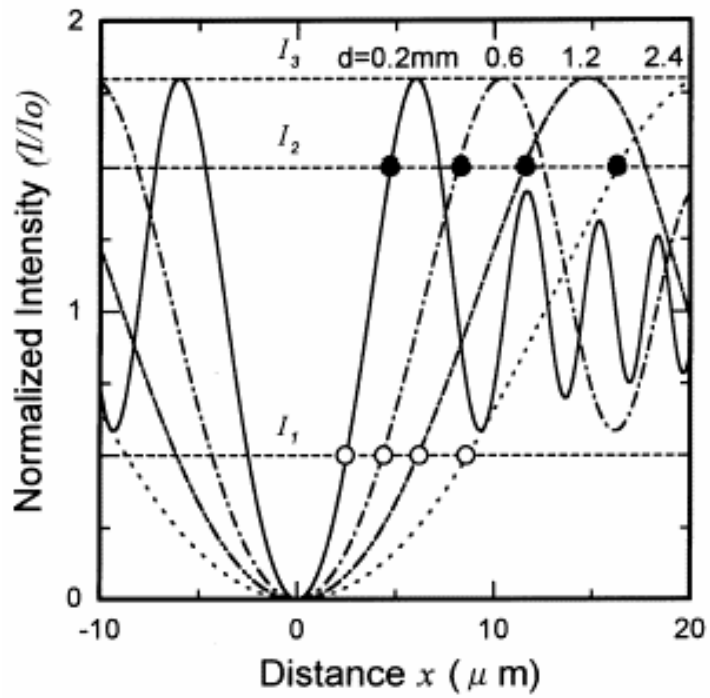


Fig. 2-16 The exhibition of the relationship between normalized intensity distributions and the distance from phase-shift mask to the sample

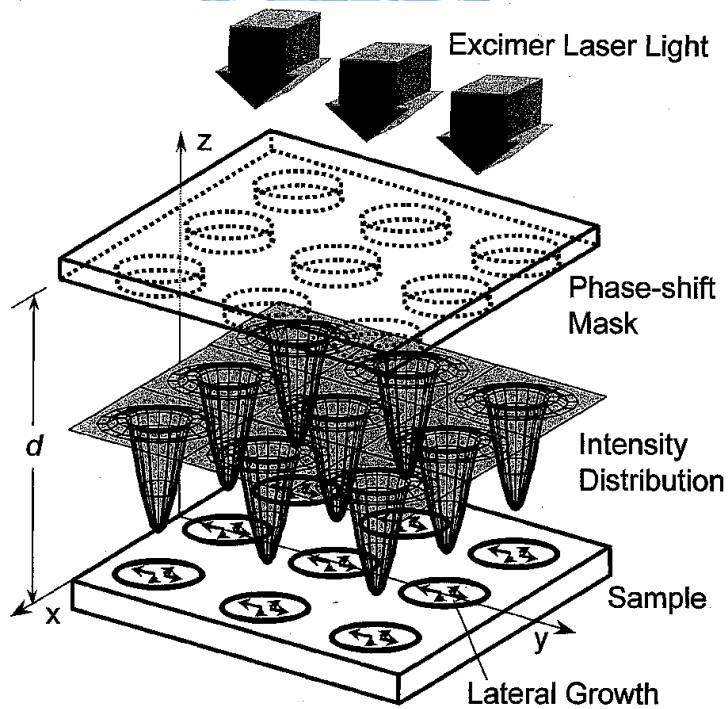


Fig. 2-17 The 2-D controlled grain growth by means of phase-shift mask

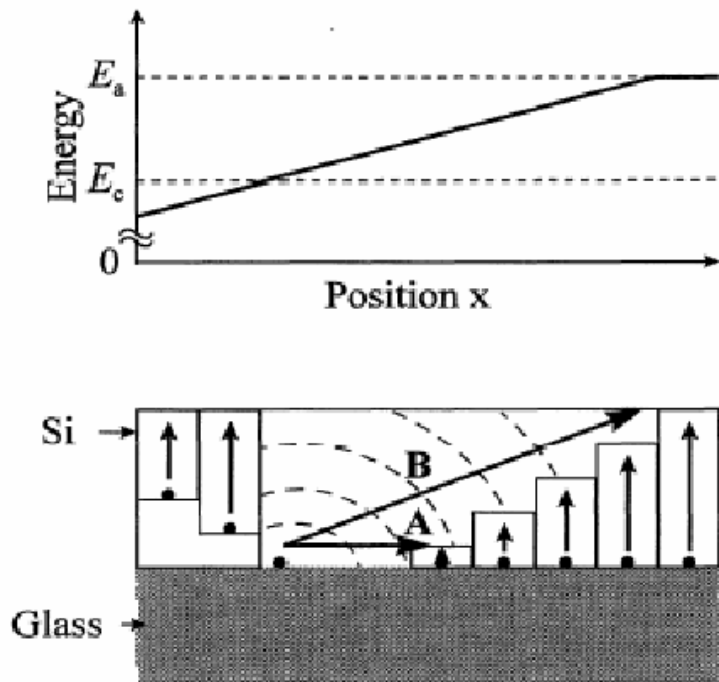


Fig. 2-18 The concept of large grain growth with graded excimer laser energy density

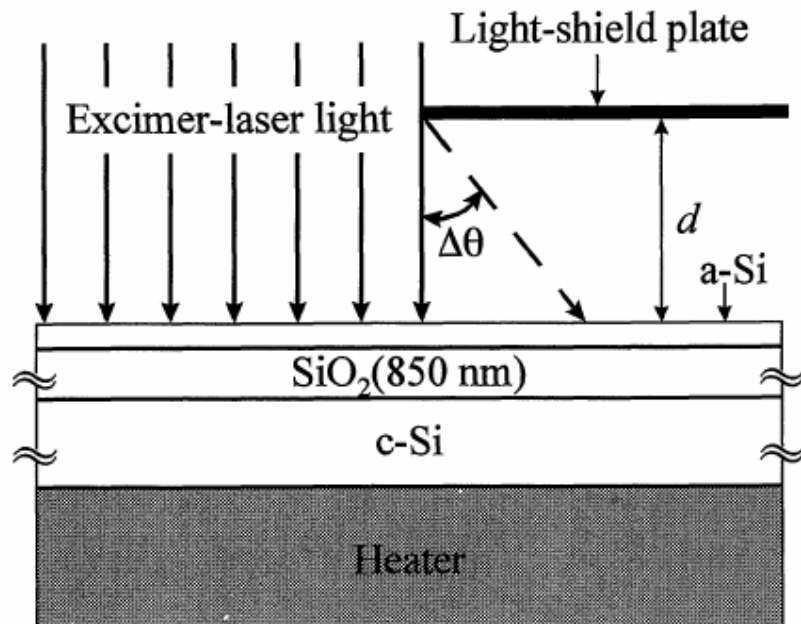


Fig. 2-19 The graded laser energy density resulted from the light-shield plate

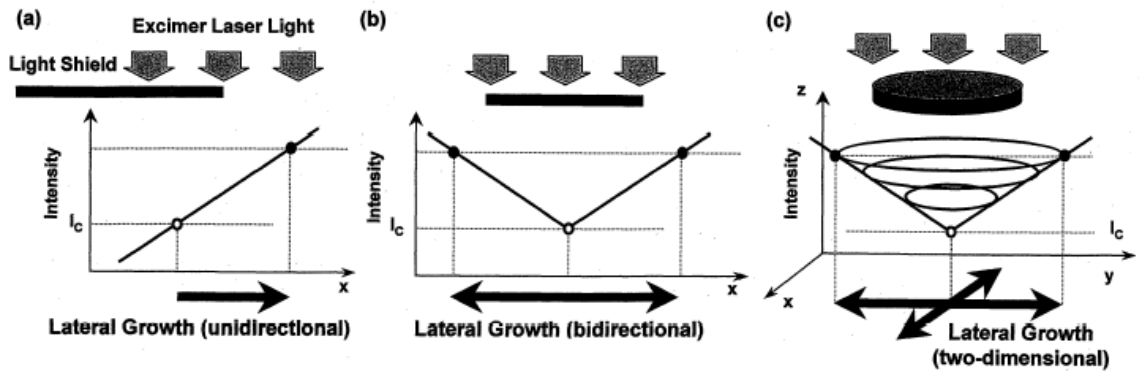
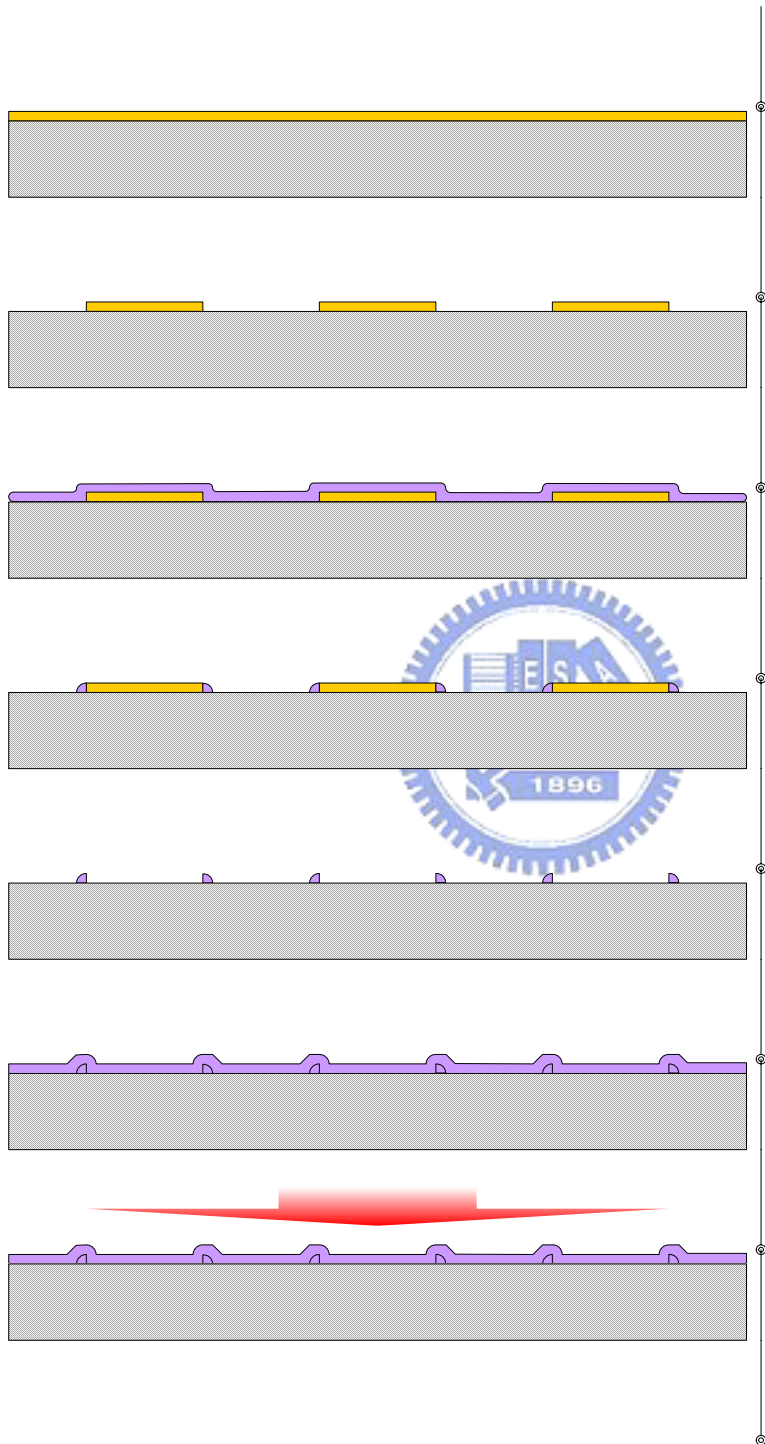


Fig. 2-20 The 2-D controlled grain growth by means of light-shield plate





Oxid

Fig. 3-1 Process flowchart of specimen preparation for material analysis

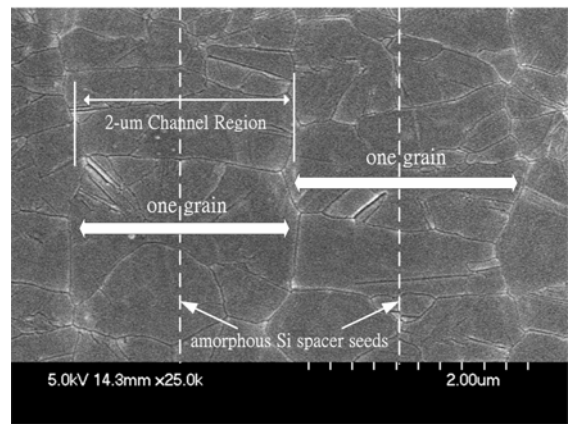
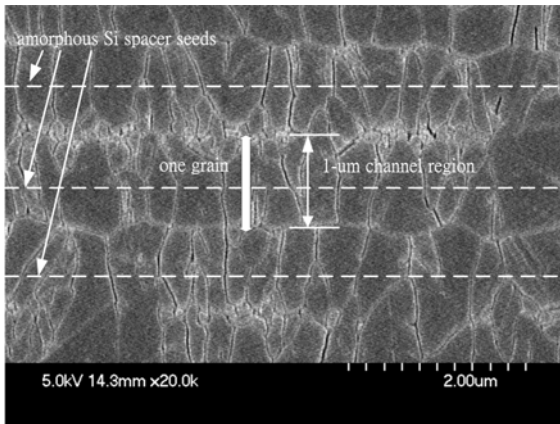


Fig. 3-2 SEM of ELC poly-Si thin film with 50nm height a-Si spacer structure

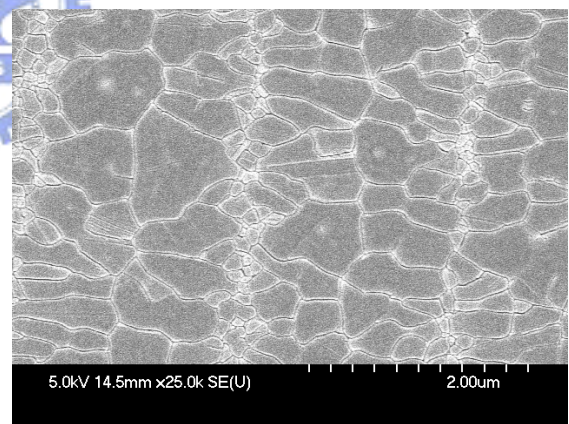
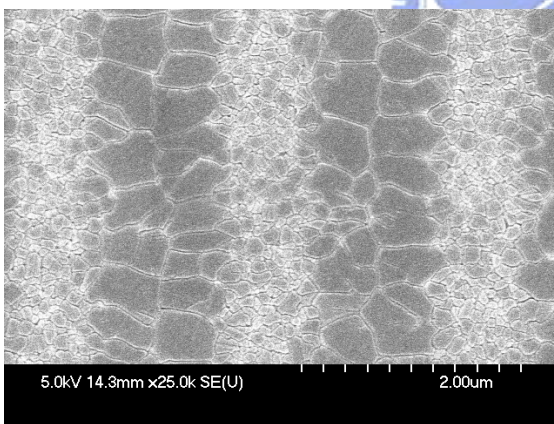


Fig. 3-3 SEM of ELC poly-Si thin film with 100nm height a-Si spacer structure

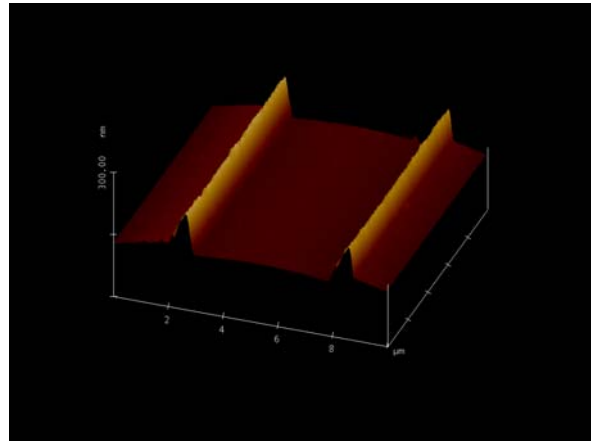
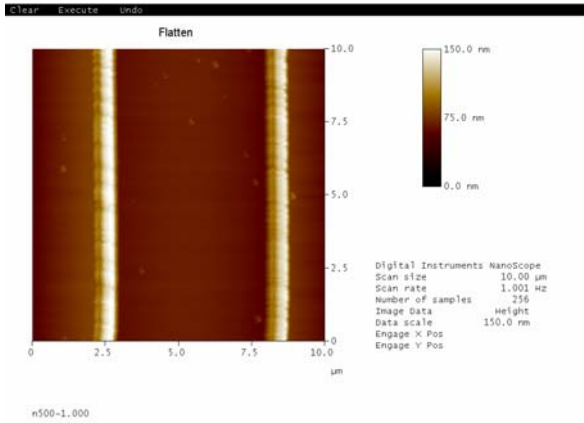


Fig. 3-4 AFM of 50nm height a-Si spacer structure

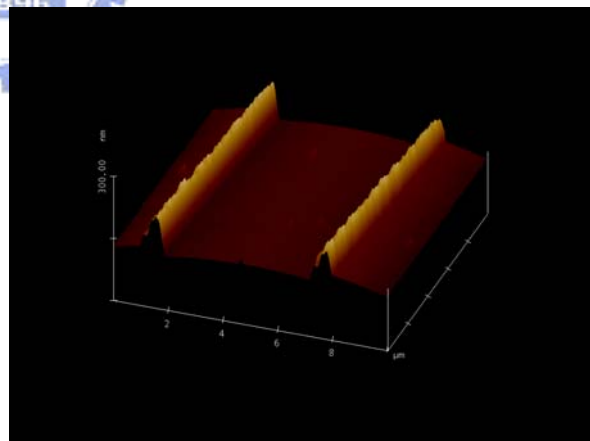
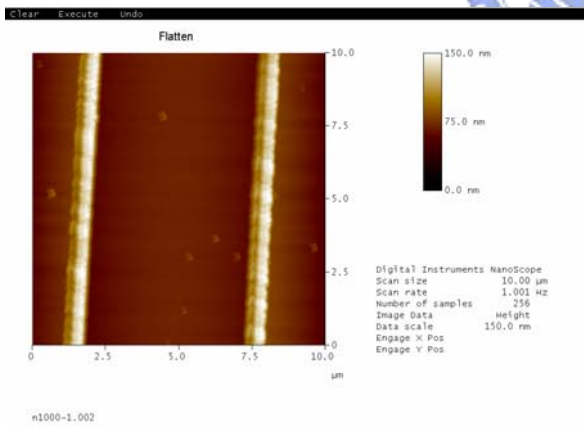


Fig. 3-5 AFM of 100nm height a-Si spacer structure

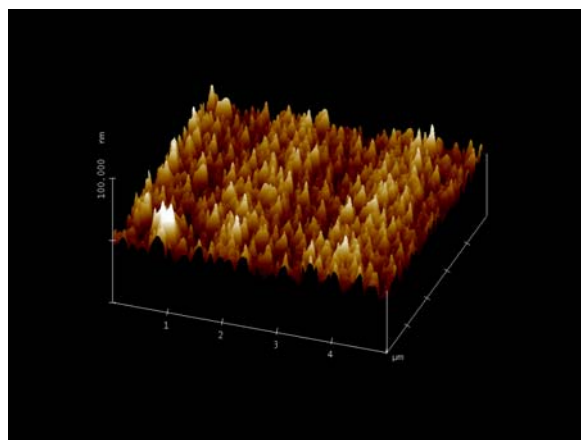
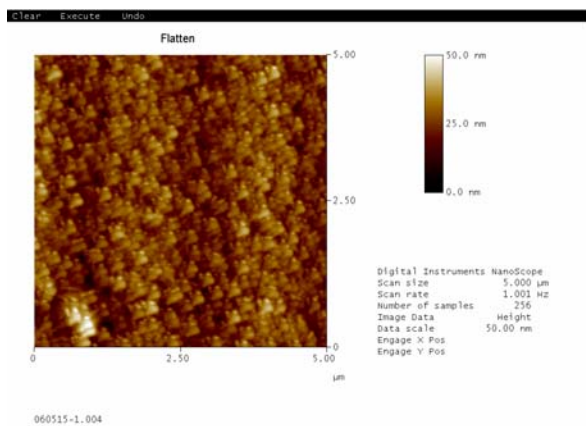


Fig. 3-6 AFM of ELC poly-Si thin film with 50nm height a-Si spacer structure

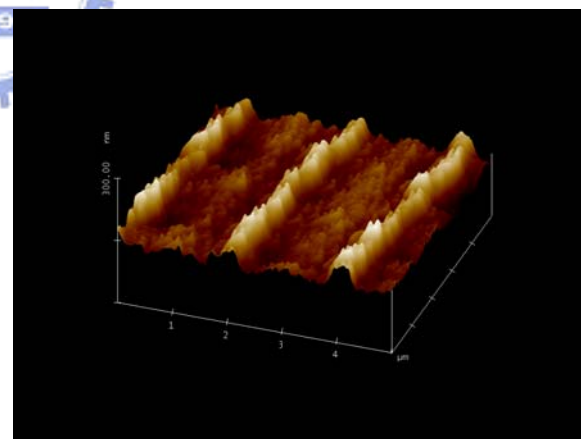
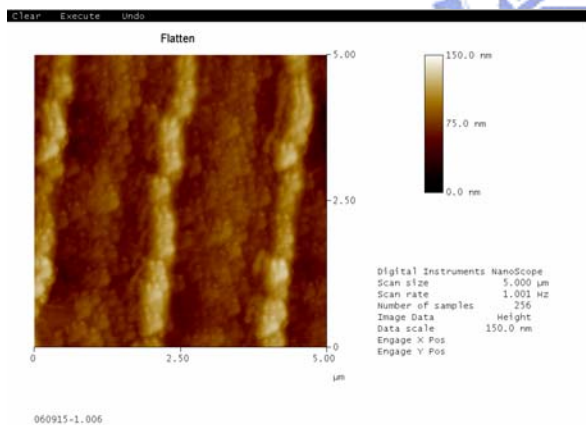


Fig. 3-7 AFM of ELC poly-Si thin film with 100nm height a-Si spacer structure

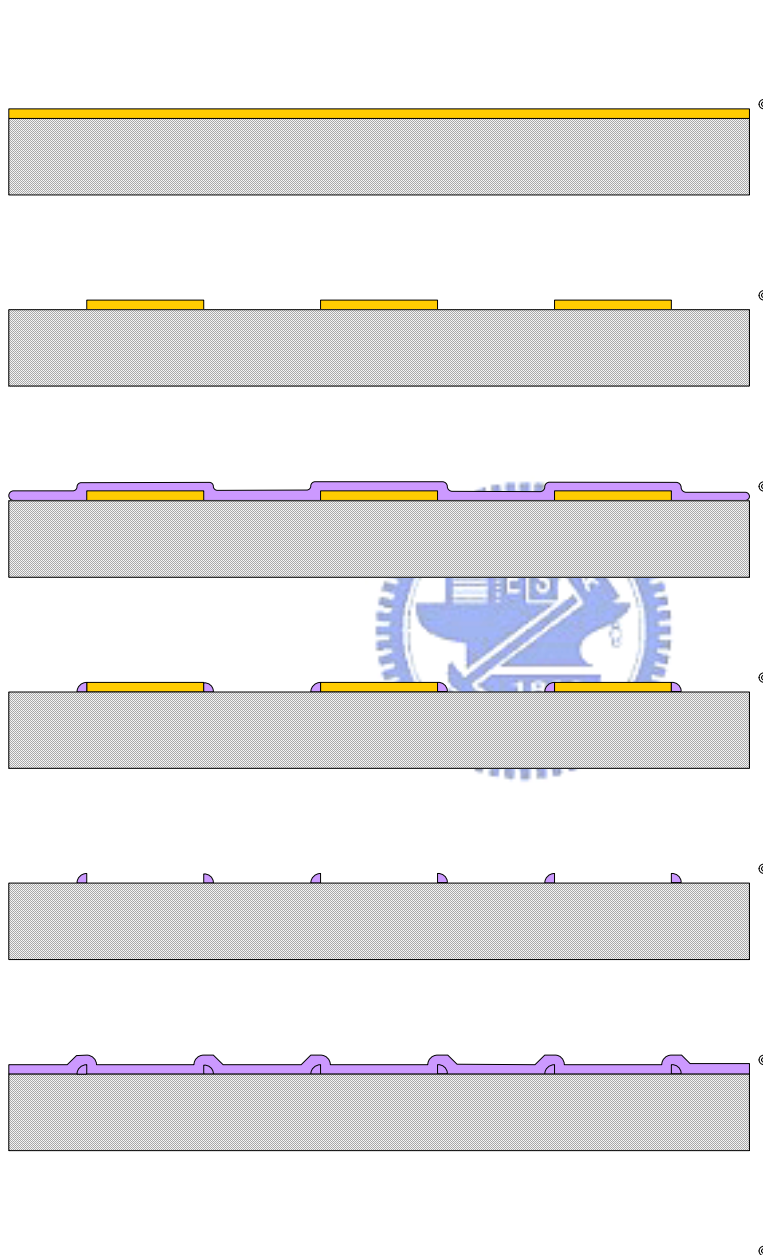
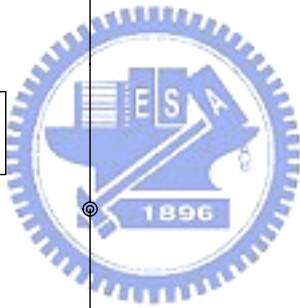
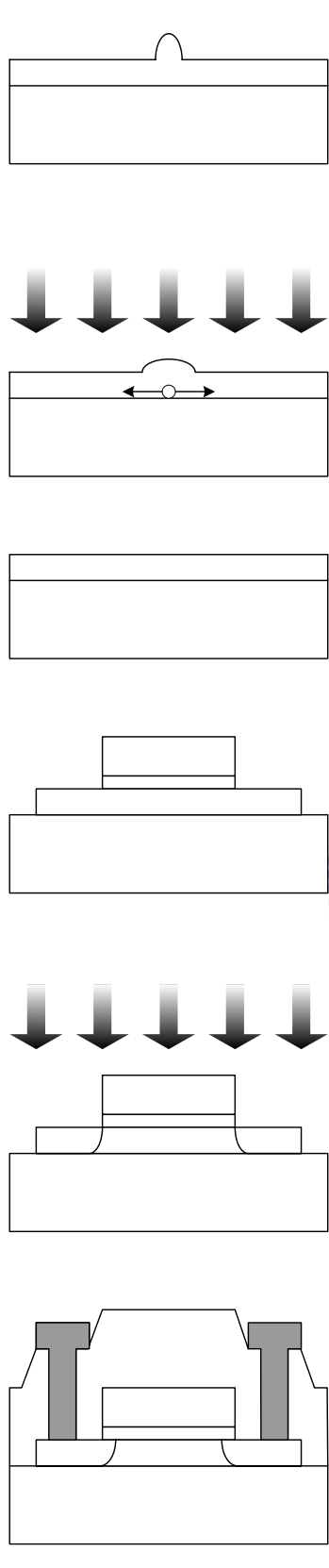


Fig. 4-1 Process flowchart of a-Si spacer structure with pre-patterned nitride layer



a-Si

Oxidized Silicon

Excimer Laser Irr

Oxidized Silicon

Fig. 4-2 Process flowchart of ELC poly-Si TFT with a-Si spacer structure

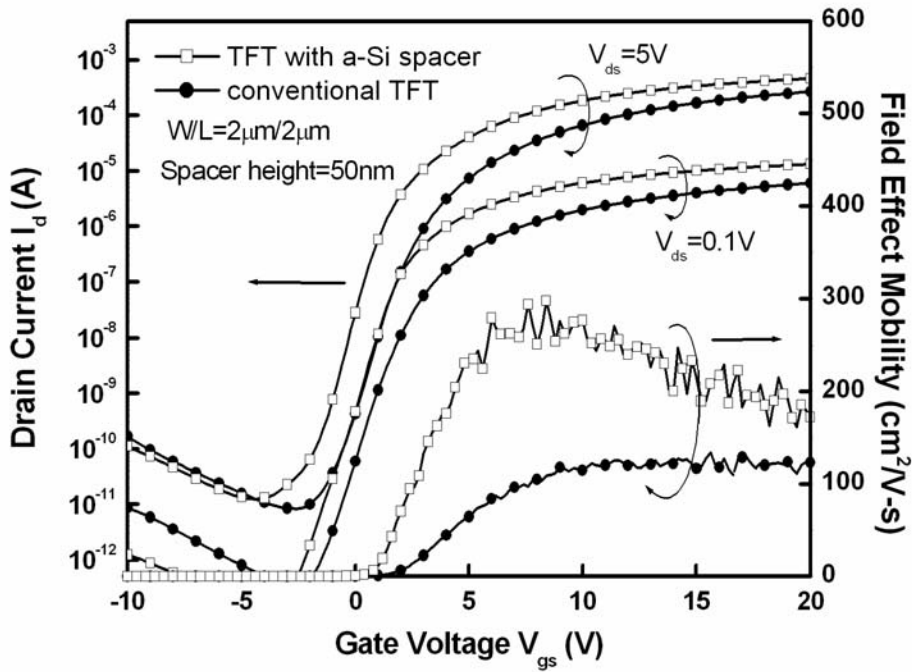


Fig. 4-3(a) Transfer characteristics of ELC poly-Si TFT with 50nm height a-Si spacer structure for $W/L=2\mu\text{m}/2\mu\text{m}$ and conventional counterpart

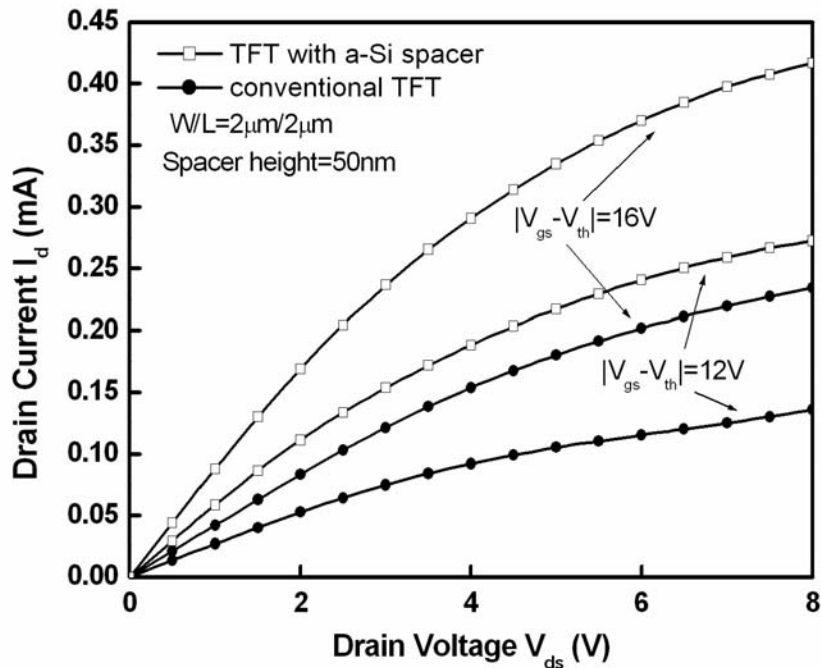


Fig. 4-3(b) Output characteristics of ELC poly-Si TFT with 50nm height a-Si spacer structure for $W/L=2\mu\text{m}/2\mu\text{m}$ and conventional counterpart

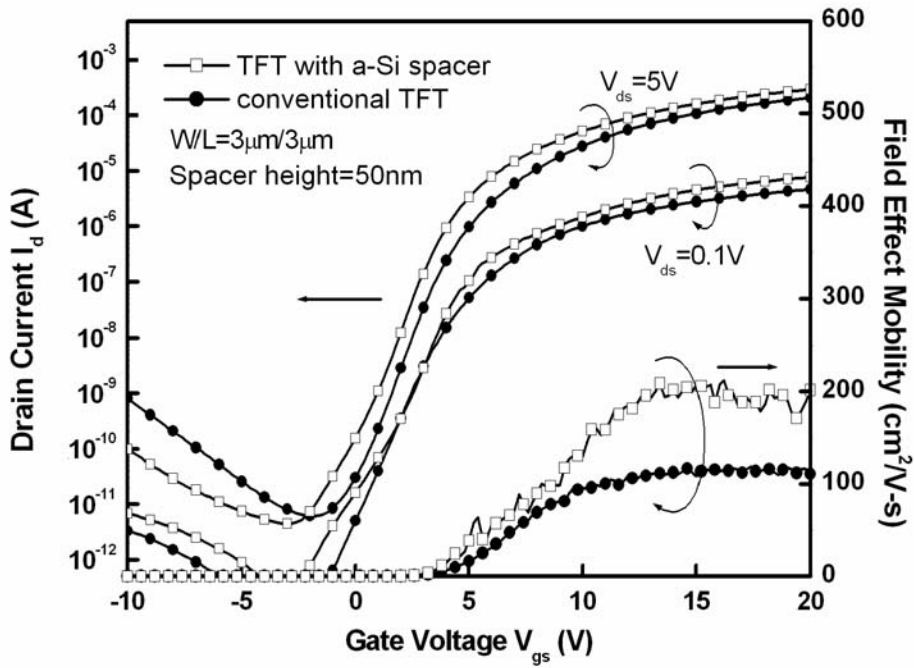


Fig. 4-4(a) Transfer characteristics of ELC poly-Si TFT with 50nm height a-Si spacer structure for $W/L=3\mu\text{m}/3\mu\text{m}$ and conventional counterpart

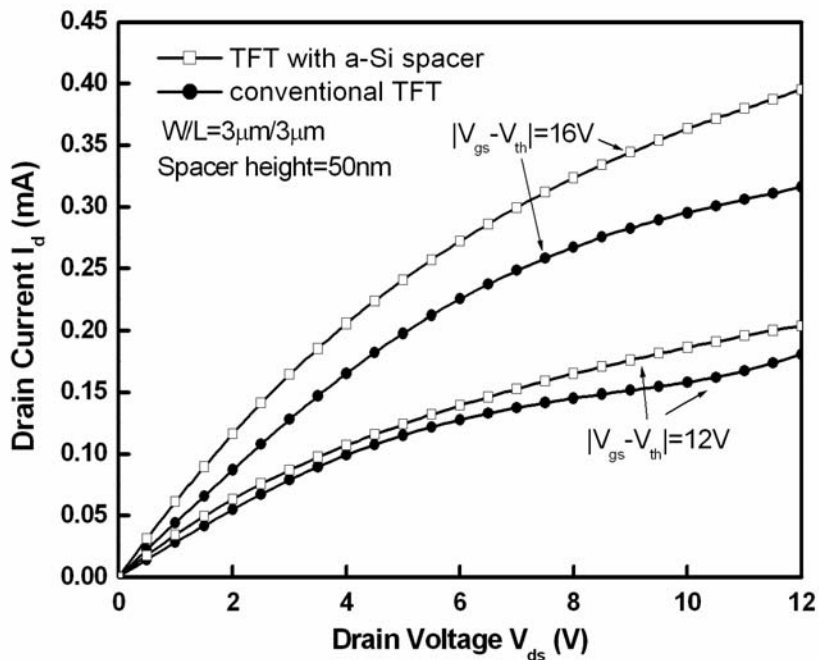


Fig. 4-4(b) Output characteristics of ELC poly-Si TFT with 50nm height a-Si spacer structure for $W/L=3\mu\text{m}/3\mu\text{m}$ and conventional counterpart

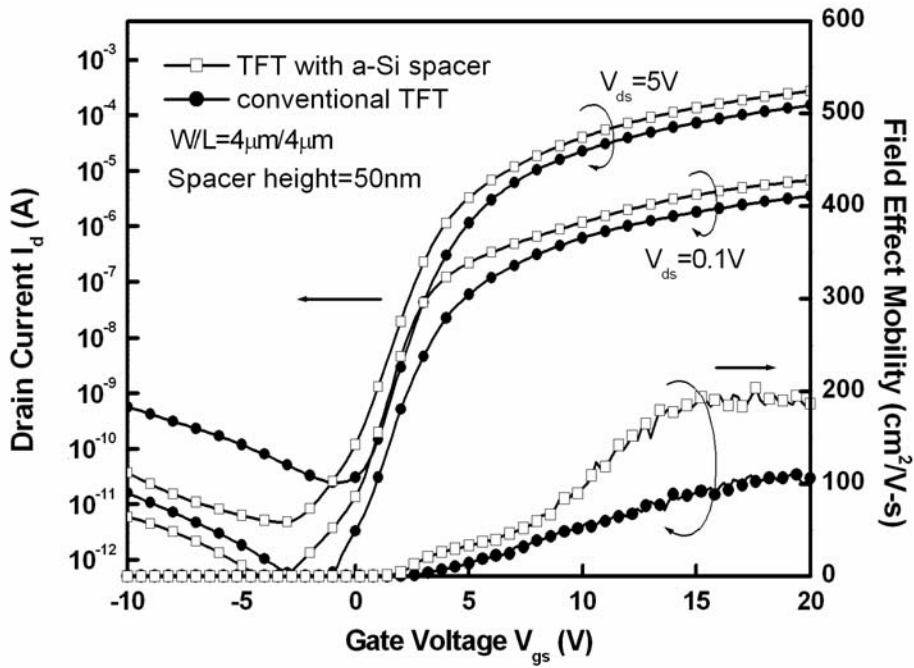


Fig. 4-5(a) Transfer characteristics of ELC poly-Si TFT with 50nm height a-Si spacer structure for $W/L=4\mu\text{m}/4\mu\text{m}$ and conventional counterpart

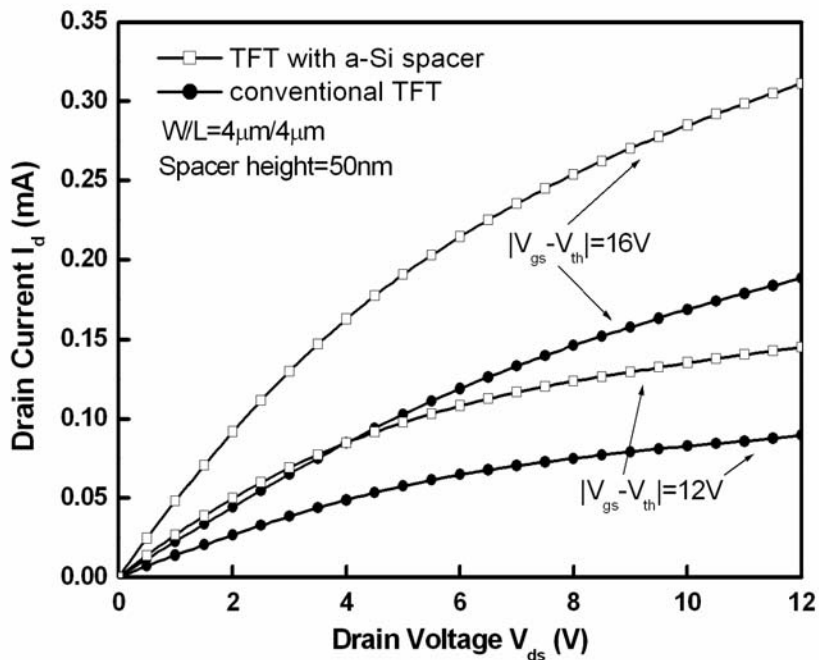


Fig. 4-5(b) Output characteristics of ELC poly-Si TFT with 50nm height a-Si spacer structure for $W/L=4\mu\text{m}/4\mu\text{m}$ and conventional counterpart

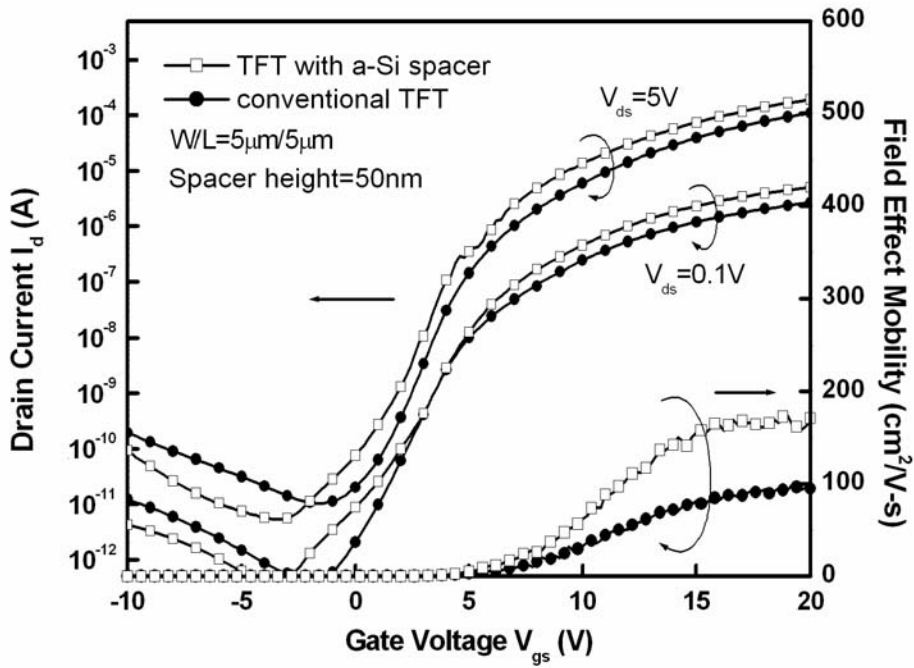


Fig. 4-6(a) Transfer characteristics of ELC poly-Si TFT with 50nm height a-Si spacer structure for $W/L=5\mu\text{m}/5\mu\text{m}$ and conventional counterpart

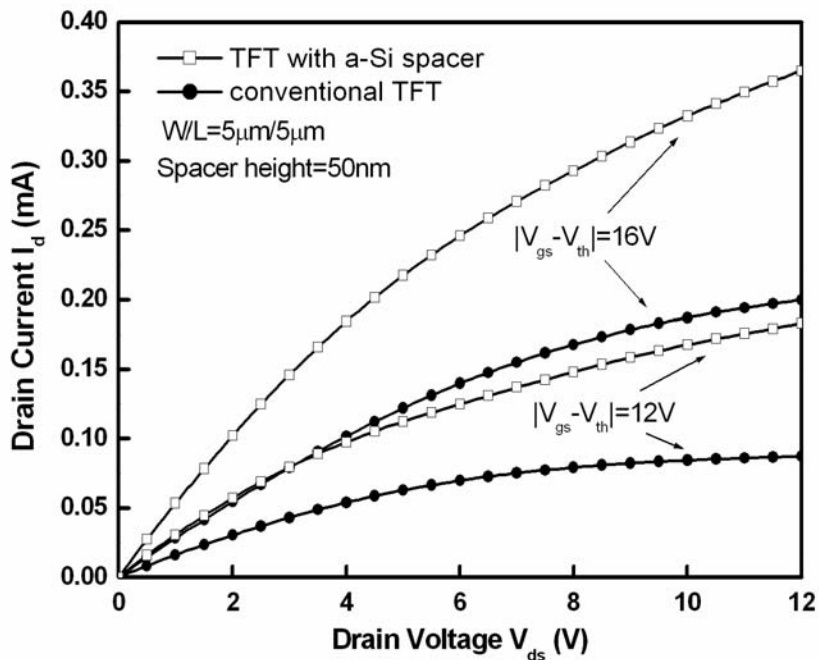


Fig. 4-6(b) Output characteristics of ELC poly-Si TFT with 50nm height a-Si spacer structure for $W/L=5\mu\text{m}/5\mu\text{m}$ and conventional counterpart

Table 4-1 Electrical characteristics of ELC poly-Si TFT with 50nm height a-Si spacer structure for different device dimension and conventional counterpart

	V_{th} (V)	Mobility (cm ² /V-s)	Sub-threshold Swing (mV/dec)	On/Off current ratio
Conventional TFT (W=L=1.5um)	-0.652	155	1072	1.68x10 ⁶
TFT with Si spacer (W=L=1.5um)	-0.438	302	807	8.68x10 ⁷
Conventional TFT (W=L=2um)	1.94	128	738	3.32x10 ⁷
TFT with Si spacer (W=L=2um)	0.976	289	672	3.68x10 ⁷
Conventional TFT (W=L=3um)	3.72	116	1010	3.41x10 ⁷
TFT with Si spacer (W=L=3um)	3.53	206	944	6.81x10 ⁷
Conventional TFT (W=L=4um)	3.44	108	779	6.23x10 ⁶
TFT with Si spacer (W=L=4um)	2.29	198	704	5.73x10 ⁷
Conventional TFT (W=L=5um)	4.99	97	1170	1.04x10 ⁷
TFT with Si spacer (W=L=5um)	4.84	169	1170	3.6x10 ⁷

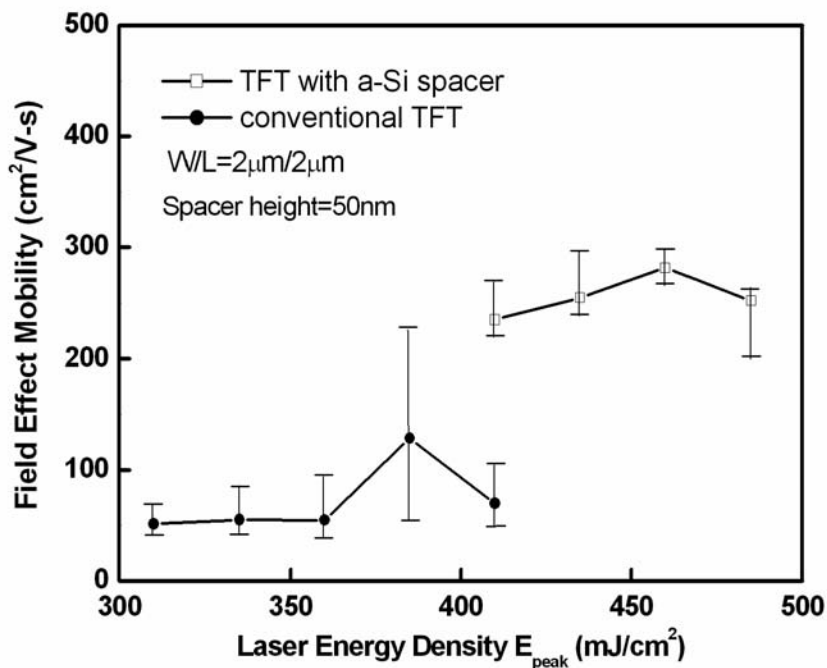


Fig. 4-7 Dependence of field effect mobility on laser energy density of ELC poly-Si TFT with 50nm height a-Si spacer structure for W/L=2µm/2µm and conventional counterpart

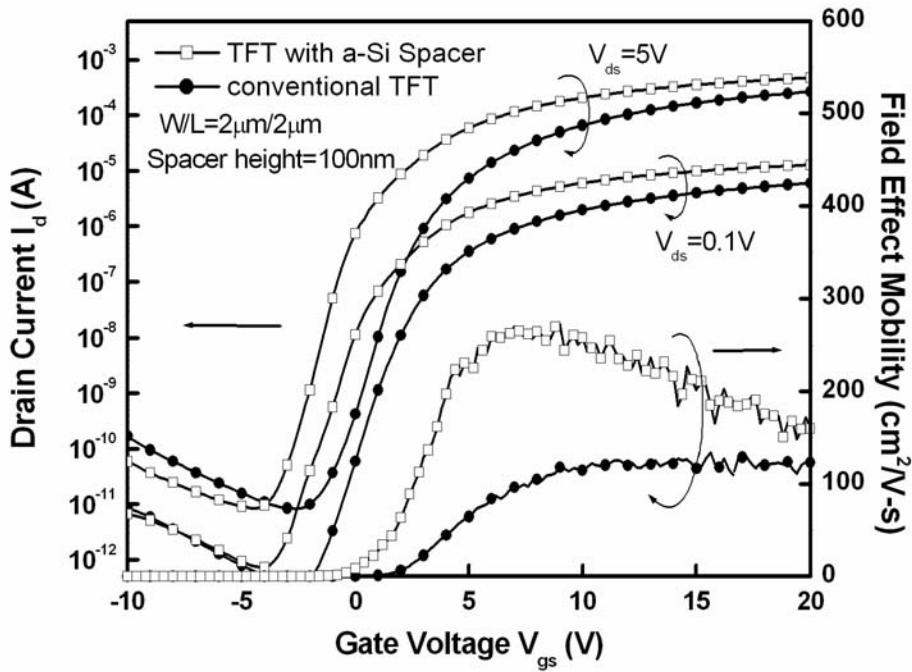


Fig. 4-8(a) Transfer characteristics of ELC poly-Si TFT with 100nm height a-Si spacer structure for $W/L=2\mu\text{m}/2\mu\text{m}$ and conventional counterpart

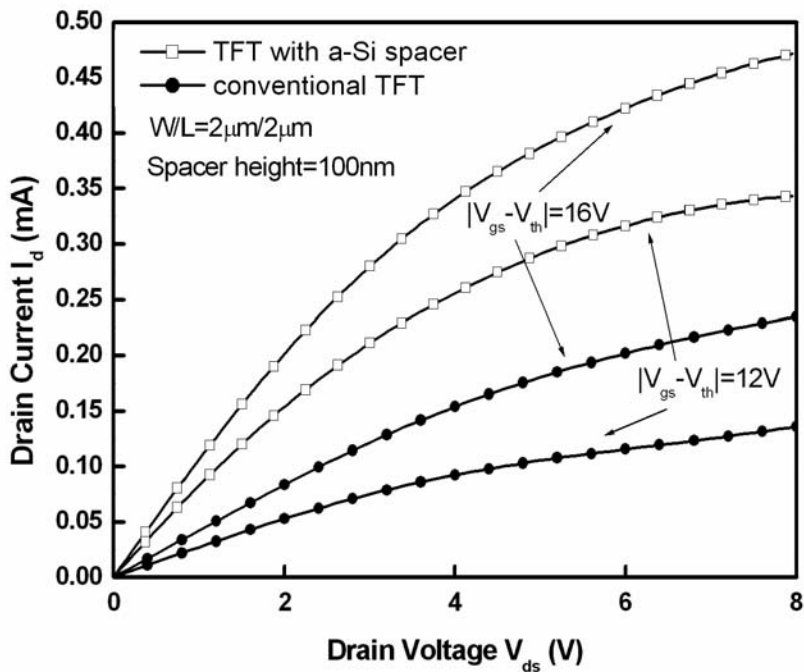


Fig. 4-8(b) Output characteristics of ELC poly-Si TFT with 100nm height a-Si spacer structure for $W/L=2\mu\text{m}/2\mu\text{m}$ and conventional counterpart

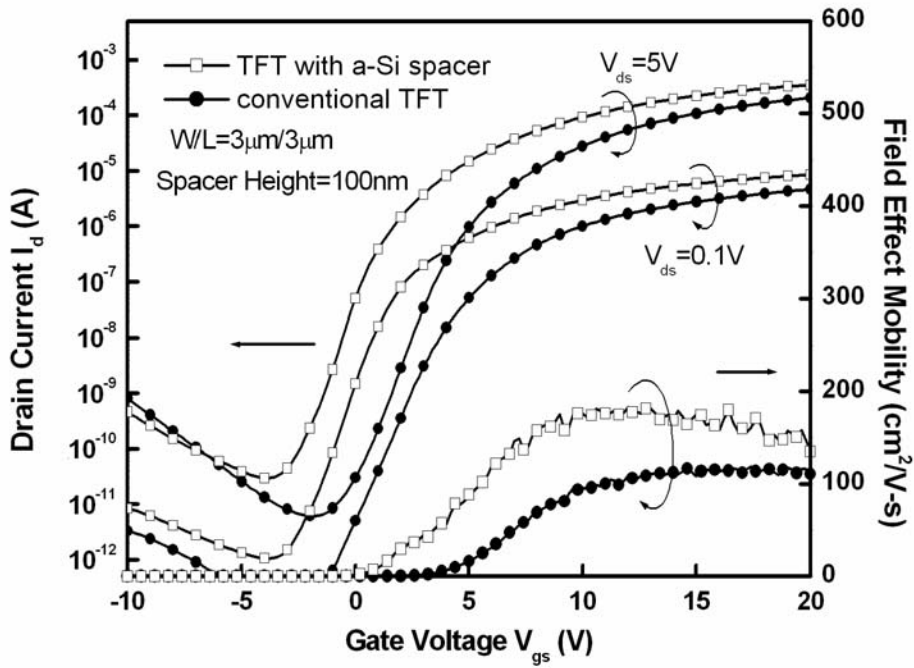


Fig. 4-9(a) Transfer characteristics of ELC poly-Si TFT with 100nm height a-Si spacer structure for $W/L=3\mu\text{m}/3\mu\text{m}$ and conventional counterpart

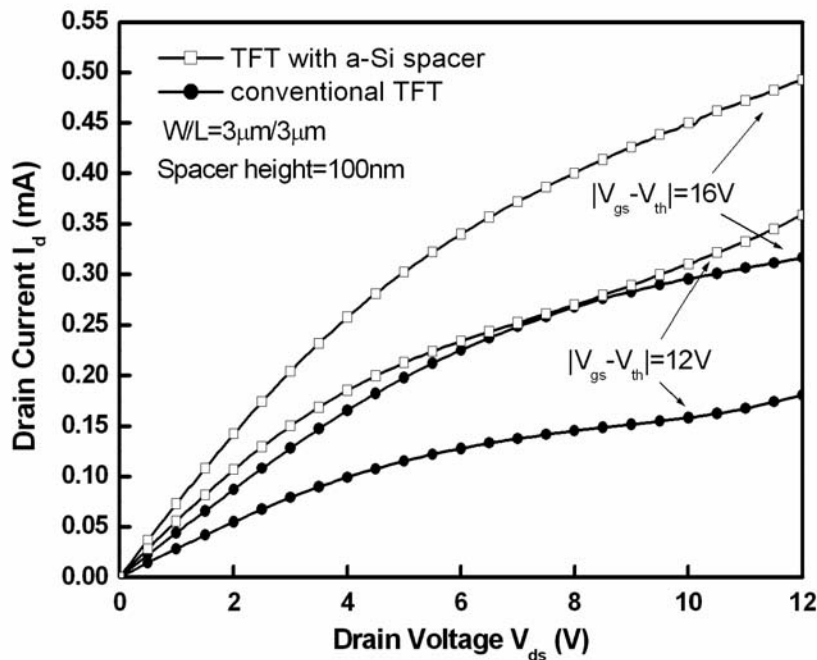


Fig. 4-9(b) Output characteristics of ELC poly-Si TFT with 100nm height a-Si spacer structure for $W/L=3\mu\text{m}/3\mu\text{m}$ and conventional counterpart

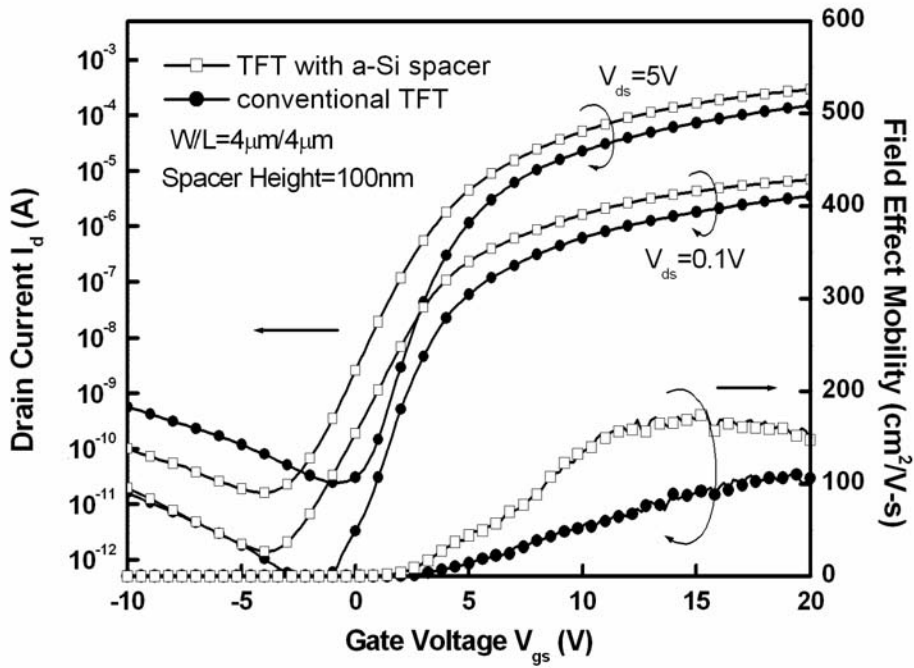


Fig. 4-10(a) Transfer characteristics of ELC poly-Si TFT with 100nm height a-Si spacer structure for $W/L=4\mu\text{m}/4\mu\text{m}$ and conventional counterpart

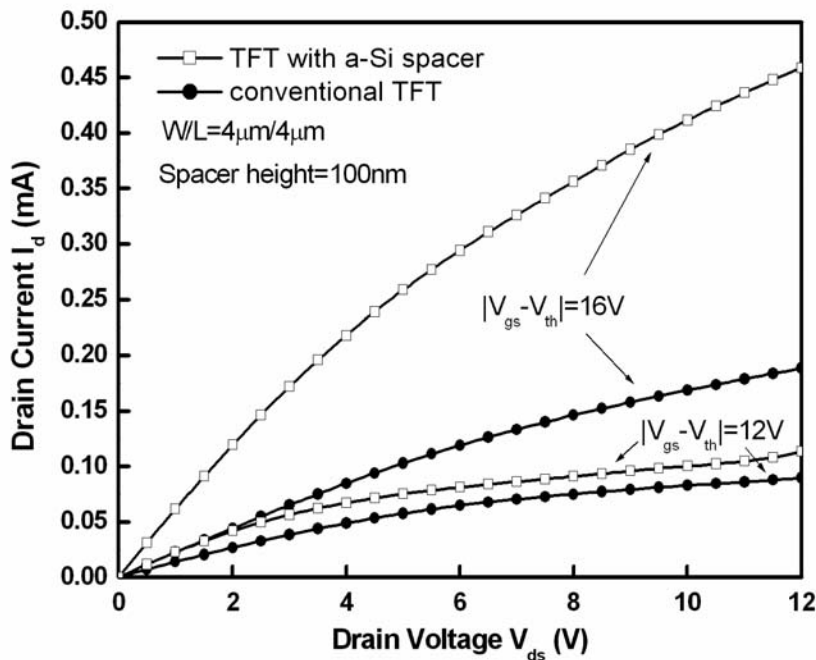


Fig. 4-10(b) Output characteristics of ELC poly-Si TFT with 100nm height a-Si spacer structure for $W/L=4\mu\text{m}/4\mu\text{m}$ and conventional counterpart

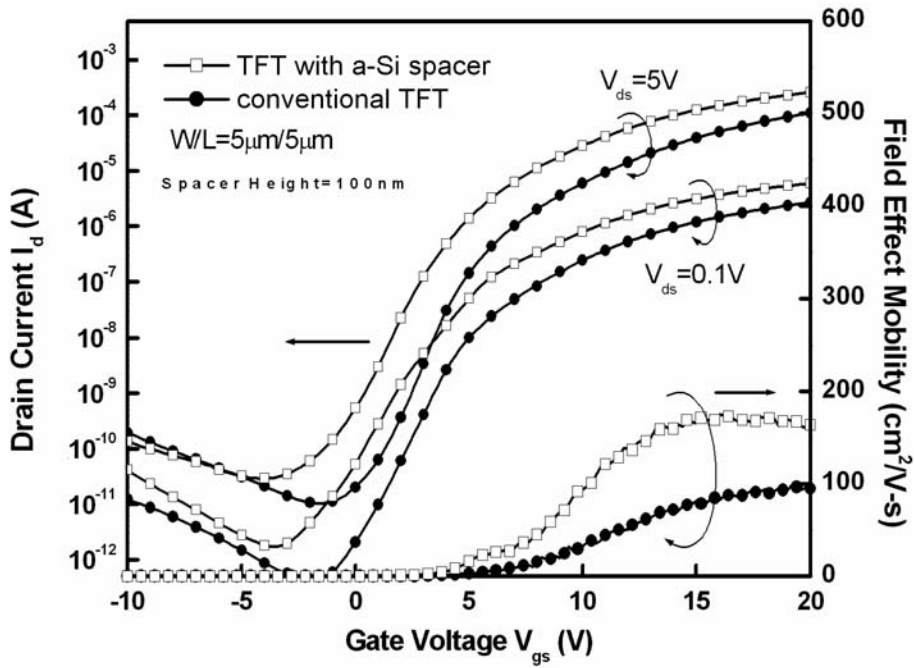


Fig. 4-11(a) Transfer characteristics of ELC poly-Si TFT with 100nm height a-Si spacer structure for $W/L=5\mu\text{m}/5\mu\text{m}$ and conventional counterpart

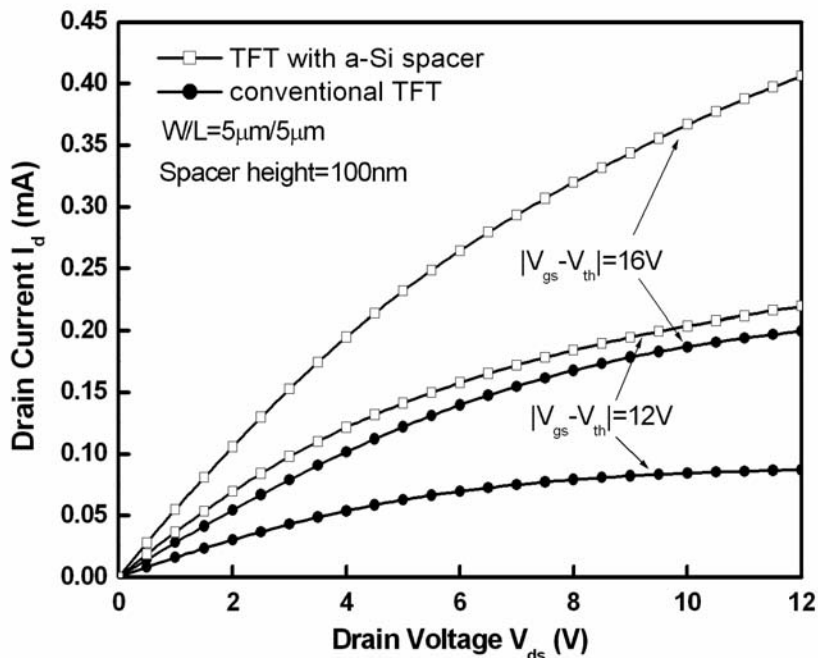


Fig. 4-11(b) Output characteristics of ELC poly-Si TFT with 100nm height a-Si spacer structure for $W/L=5\mu\text{m}/5\mu\text{m}$ and conventional counterpart

Table 4-2 Electrical characteristics of ELC poly-Si TFT with 100nm height a-Si spacer structure for different device dimension and conventional counterpart

	V_{th} (V)	Mobility (cm ² /V-s)	Sub-threshold Swing (mV/dec)	On/Off current ratio
Conventional TFT (W=L=1.5um)	-0.652	155	1072	1.68x10 ⁶
TFT with Si spacer (W=L=1.5um)	-0.246	258	546	2.25x10 ⁷
Conventional TFT (W=L=2um)	1.94	128	738	3.32x10 ⁷
TFT with Si spacer (W=L=2um)	-0.051	265	713	5.59x10 ⁷
Conventional TFT (W=L=3um)	3.72	116	1010	3.41x10 ⁷
TFT with Si spacer (W=L=3um)	0.787	189	786	1.20x10 ⁷
Conventional TFT (W=L=4um)	3.44	108	779	6.23x10 ⁶
TFT with Si spacer (W=L=4um)	2.53	174	1247	5.86x10 ⁶
Conventional TFT (W=L=5um)	4.99	97	1170	1.04x10 ⁷
TFT with Si spacer (W=L=5um)	4.1	170	1442	9.48x10 ⁶

Table 4-3 Electrical characteristics of ELC poly-Si TFT with 50nm and 100nm height a-Si spacer structure for different device dimension

	V_{th} (V)	Mobility (cm ² /V-s)	Sub-threshold Swing (mV/dec)	On/Off current ratio
Nitride = 500Å (W=L=1.5um)	-0.438	302	807	8.68x10 ⁷
Nitride = 1000Å (W=L=1.5um)	-0.246	258	546	2.25x10 ⁷
Nitride = 500Å (W=L=2um)	0.976	289	672	3.68x10 ⁷
Nitride = 1000Å (W=L=2um)	-0.051	265	713	5.59x10 ⁷
Nitride = 500Å (W=L=3um)	3.53	206	944	6.81x10 ⁷
Nitride = 1000Å (W=L=3um)	0.787	189	786	1.20x10 ⁷
Nitride = 500Å (W=L=4um)	2.29	198	704	5.73x10 ⁷
Nitride = 1000Å (W=L=4um)	2.53	174	1247	5.86x10 ⁶
Nitride = 500Å (W=L=5um)	4.84	169	1170	3.60x10 ⁷
Nitride = 1000Å (W=L=5um)	4.1	170	1442	9.48x10 ⁶

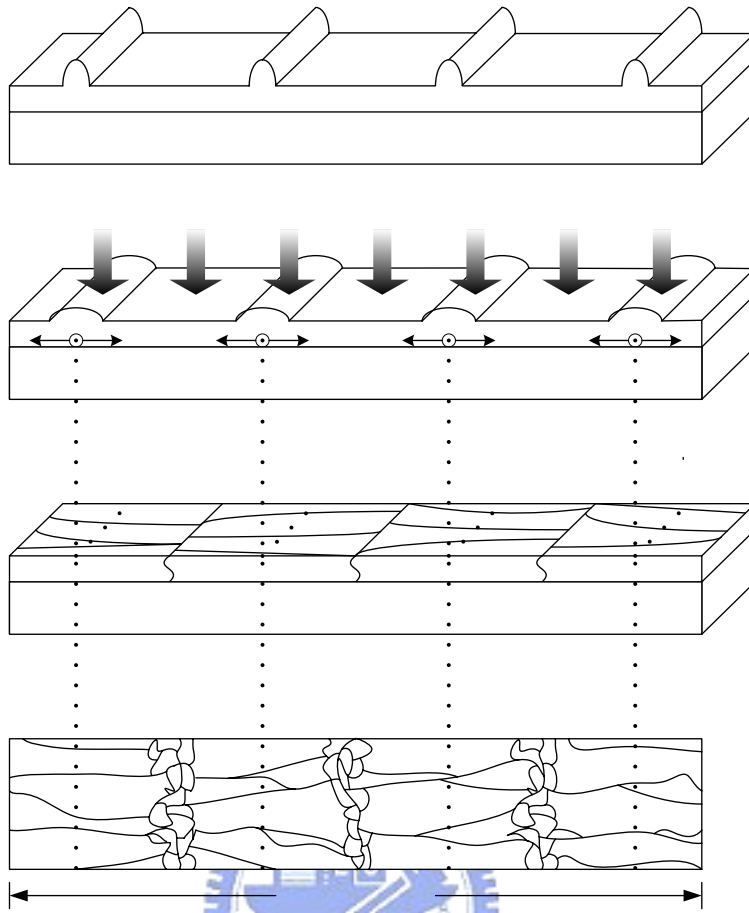


Fig. 4-12(a) The diagram of periodic grain growth for large dimension devices applications

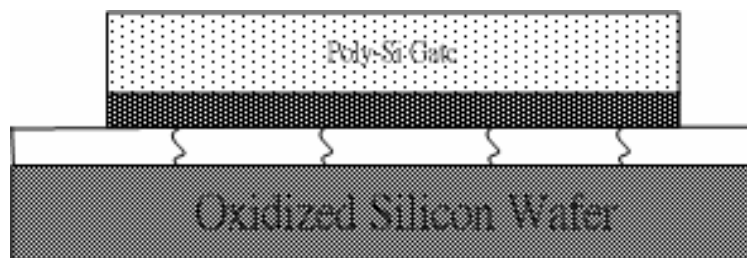


Fig. 4-12(b) The periodic grain growth for large dimension devices after gate electrode formation

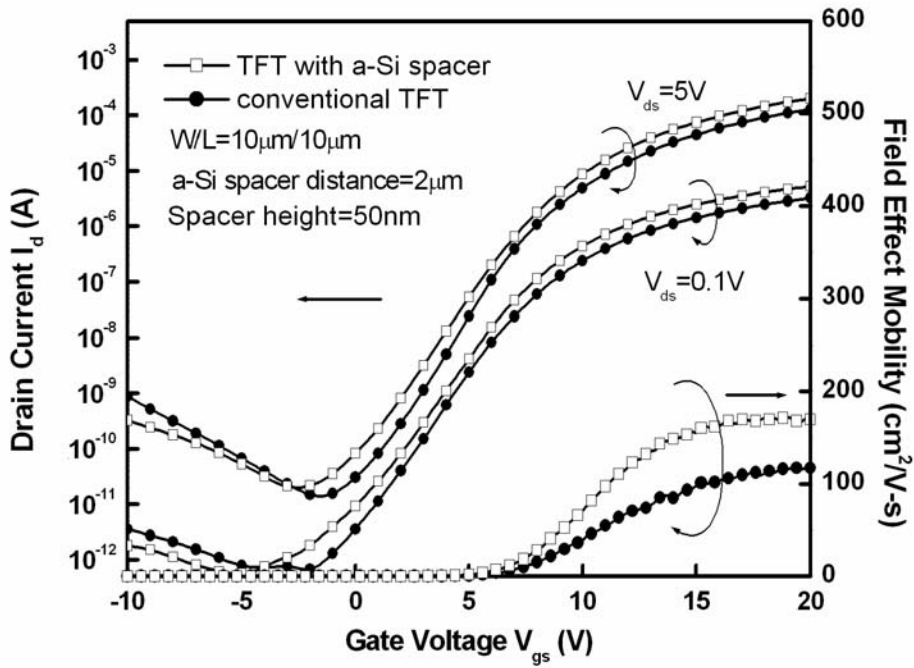


Fig. 4-13(a) Transfer characteristics of ELC poly-Si TFT with 50nm height and $2\mu\text{m}$ distance a-Si spacer structure for $W/L=10\mu\text{m}/10\mu\text{m}$ and conventional counterpart

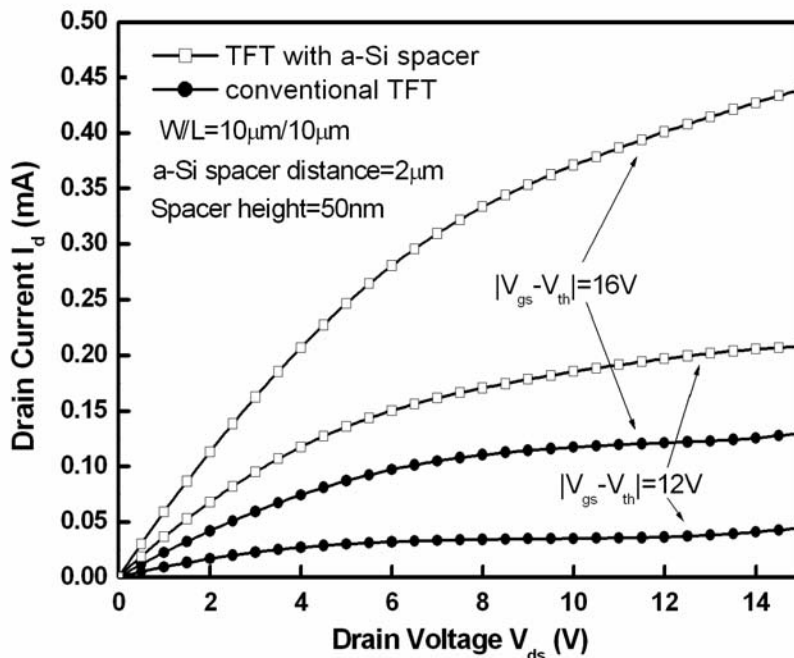


Fig. 4-13(b) Output characteristics of ELC poly-Si TFT with 50nm height and $2\mu\text{m}$ distance a-Si spacer structure for $W/L=10\mu\text{m}/10\mu\text{m}$ and conventional counterpart

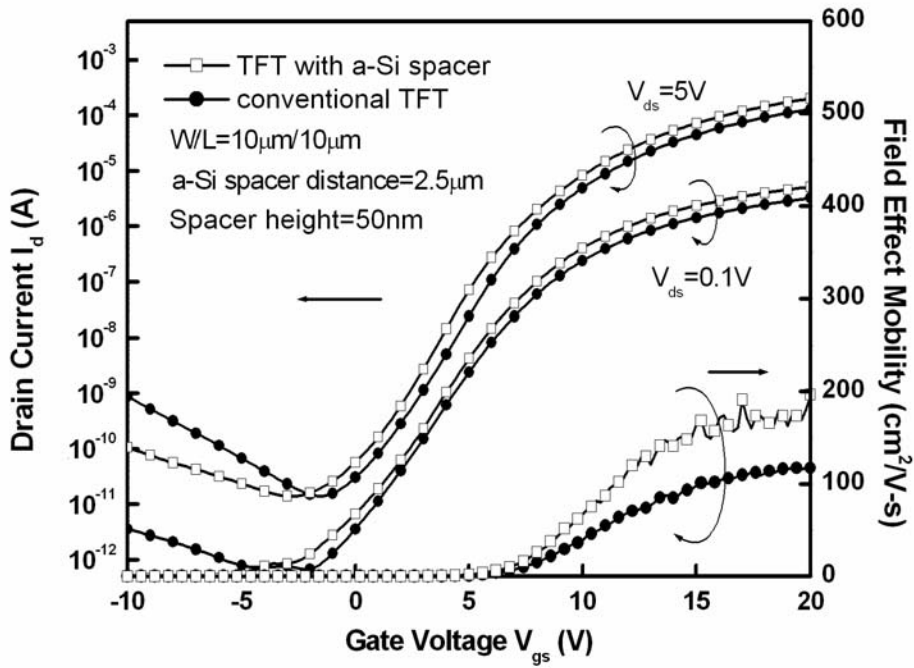


Fig. 4-14(a) Transfer characteristics of ELC poly-Si TFT with 50nm height and 2.5 μ m distance a-Si spacer structure for W/L=10 μ m/10 μ m and conventional counterpart

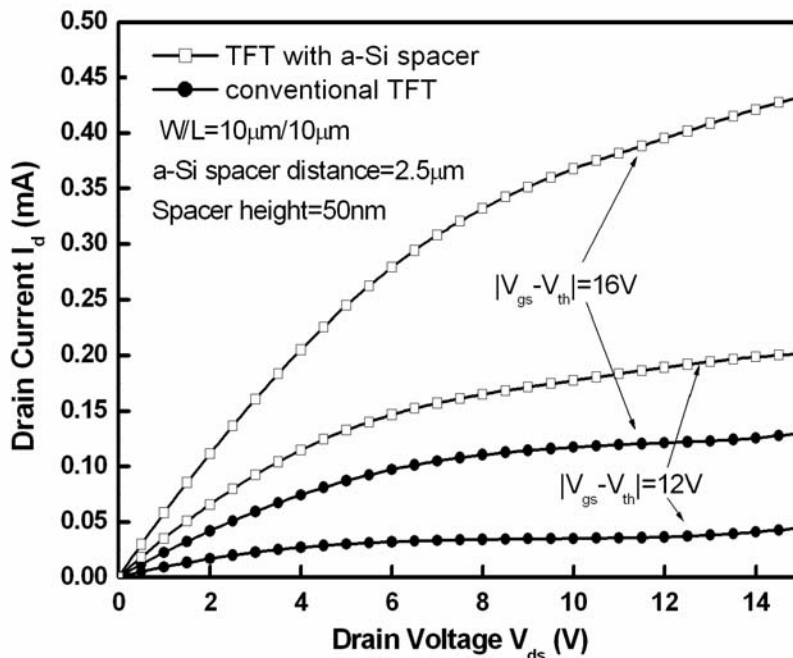


Fig. 4-14(b) Output characteristics of ELC poly-Si TFT with 50nm height and 2.5 μ m distance a-Si spacer structure for W/L=10 μ m/10 μ m and conventional counterpart

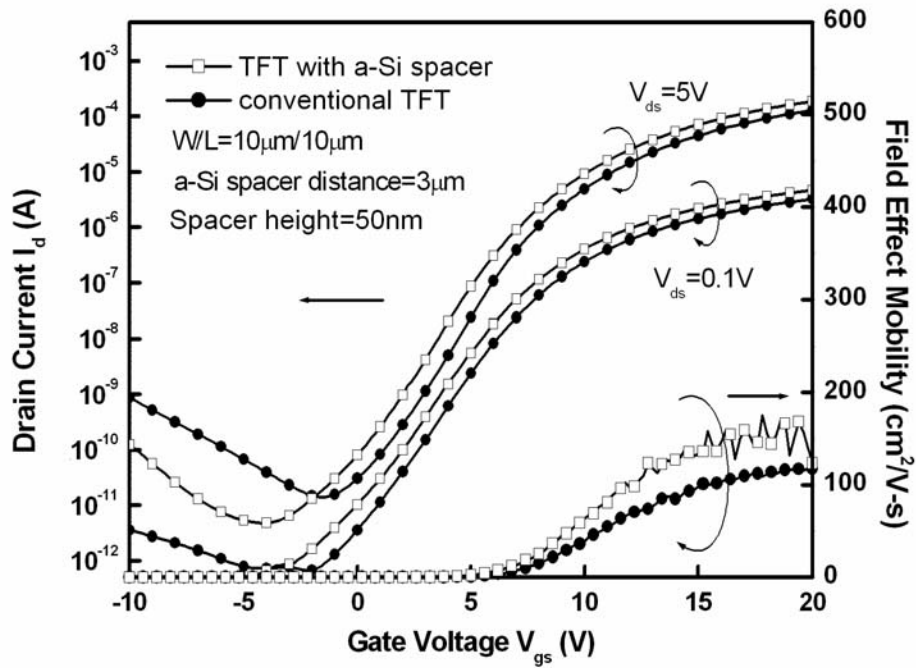


Fig. 4-15(a) Transfer characteristics of ELC poly-Si TFT with 50nm height and 3 μ m distance a-Si spacer structure for W/L=10 μ m/10 μ m and conventional counterpart

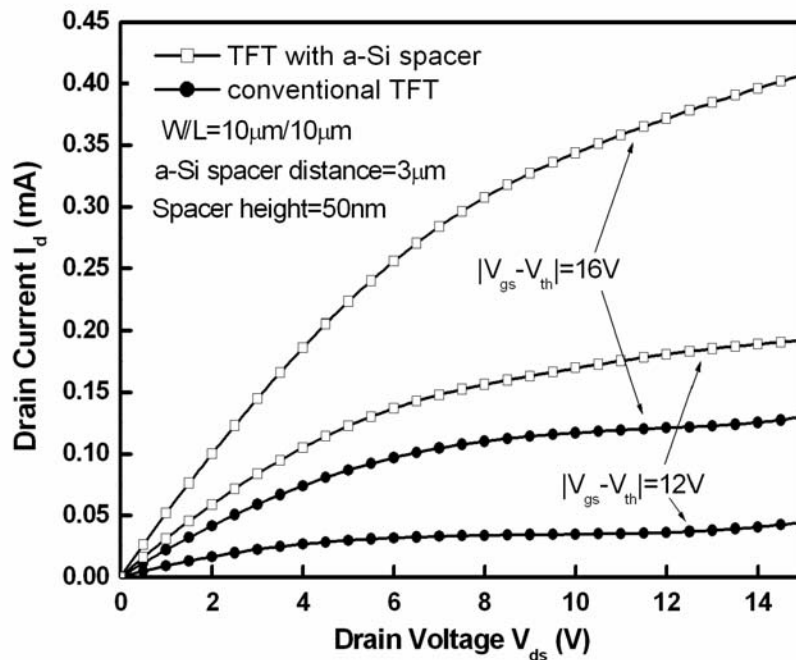


Fig. 4-15(b) Output characteristics of ELC poly-Si TFT with 50nm height and 3 μ m distance a-Si spacer structure for W/L=10 μ m/10 μ m and conventional counterpart

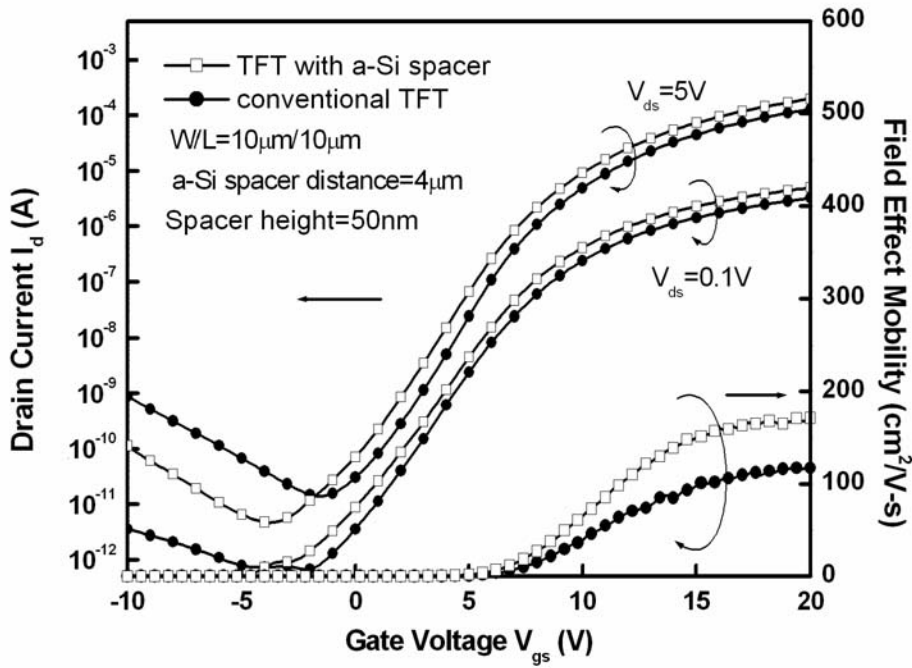


Fig. 4-16(a) Transfer characteristics of ELC poly-Si TFT with 50nm height and 4 μ m distance a-Si spacer structure for W/L=10 μ m/10 μ m and conventional counterpart

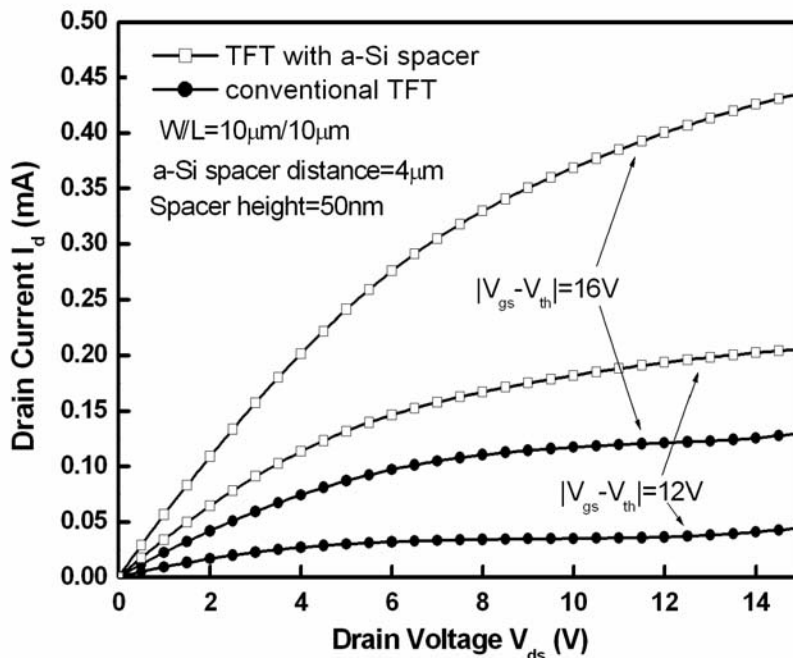


Fig. 4-16(b) Output characteristics of ELC poly-Si TFT with 50nm height and 4 μ m distance a-Si spacer structure for W/L=10 μ m/10 μ m and conventional counterpart

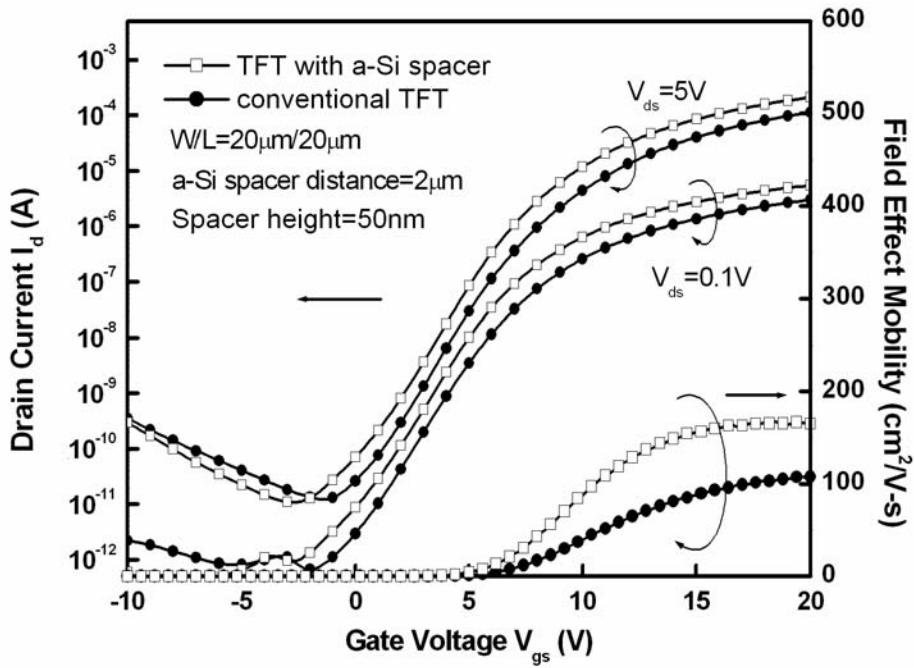


Fig. 4-17(a) Transfer characteristics of ELC poly-Si TFT with 50nm height and 2 μ m distance a-Si spacer structure for W/L=20 μ m/20 μ m and conventional counterpart

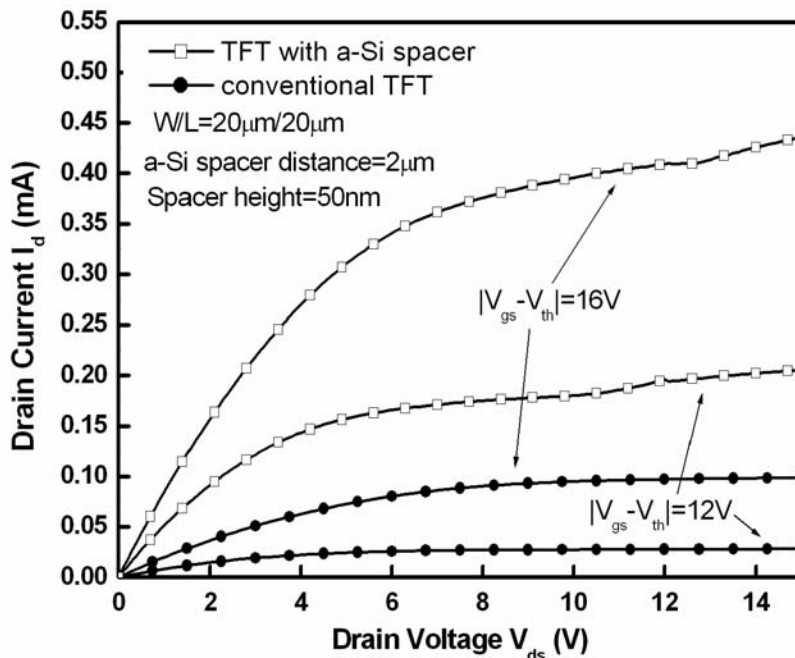


Fig. 4-17(b) Output characteristics of ELC poly-Si TFT with 50nm height and 2 μ m distance a-Si spacer structure for W/L=20 μ m/20 μ m and conventional counterpart

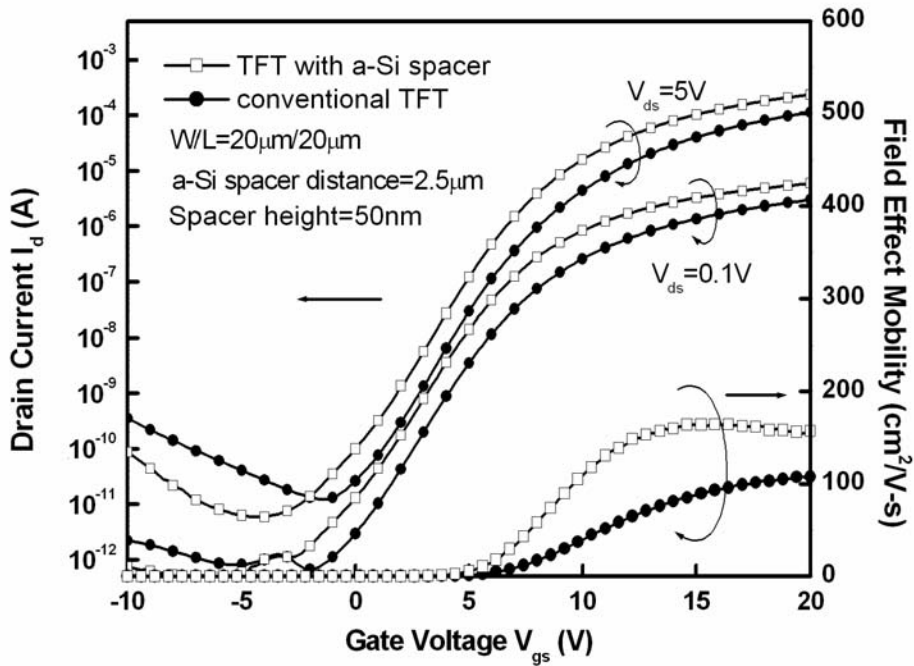


Fig. 4-18(a) Transfer characteristics of ELC poly-Si TFT with 50nm height and $2.5\mu\text{m}$ distance a-Si spacer structure for $W/L=20\mu\text{m}/20\mu\text{m}$ and conventional counterpart

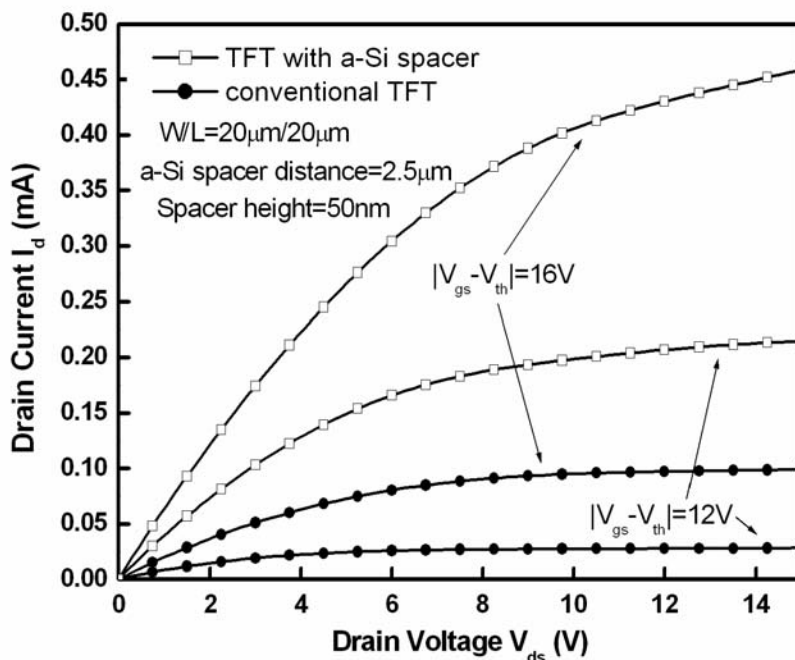


Fig. 4-18(b) Output characteristics of ELC poly-Si TFT with 50nm height and $2.5\mu\text{m}$ distance a-Si spacer structure for $W/L=20\mu\text{m}/20\mu\text{m}$ and conventional counterpart

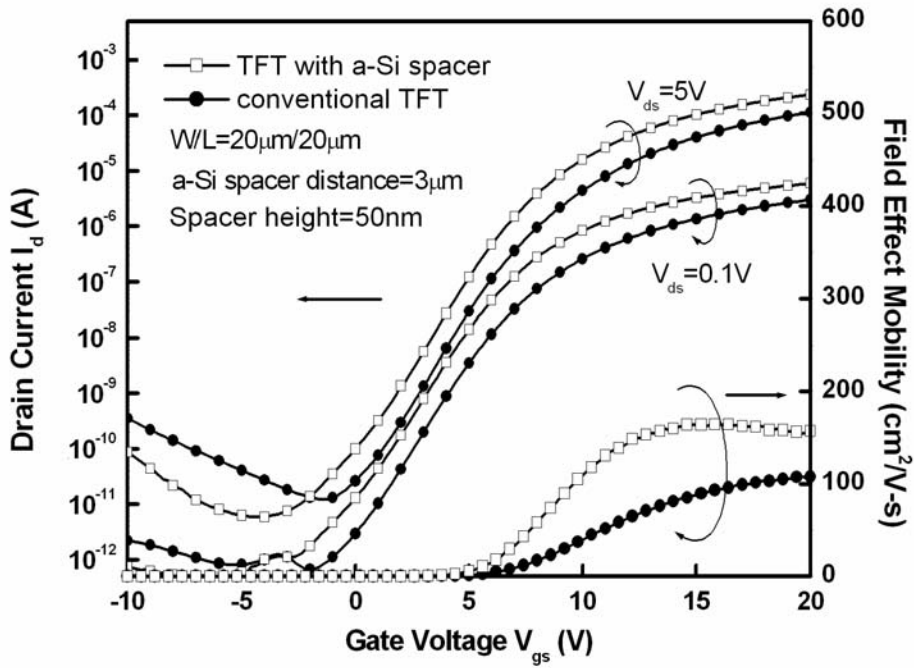


Fig. 4-19(a) Transfer characteristics of ELC poly-Si TFT with 50nm height and 3 μ m distance a-Si spacer structure for W/L=20 μ m/20 μ m and conventional counterpart

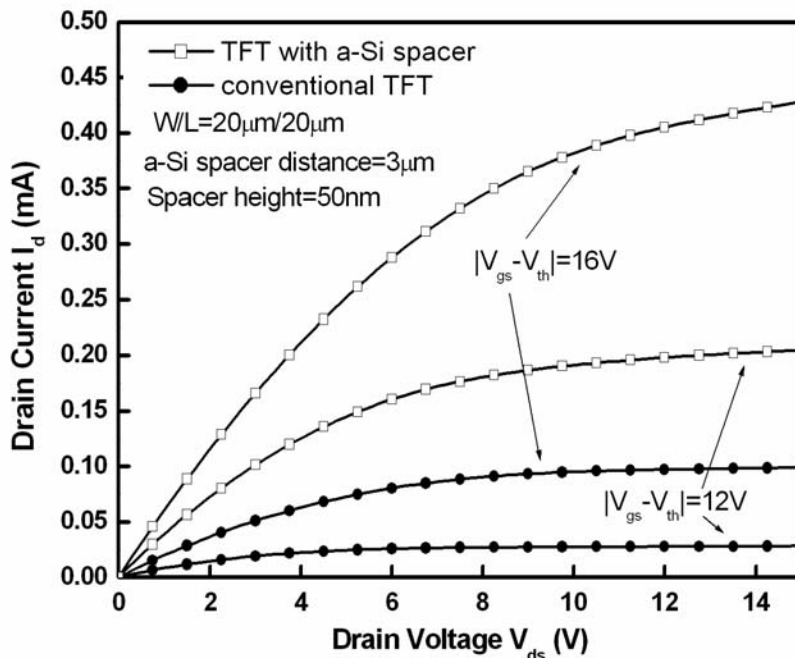


Fig. 4-19(b) Output characteristics of ELC poly-Si TFT with 50nm height and 3 μ m distance a-Si spacer structure for W/L=20 μ m/20 μ m and conventional counterpart

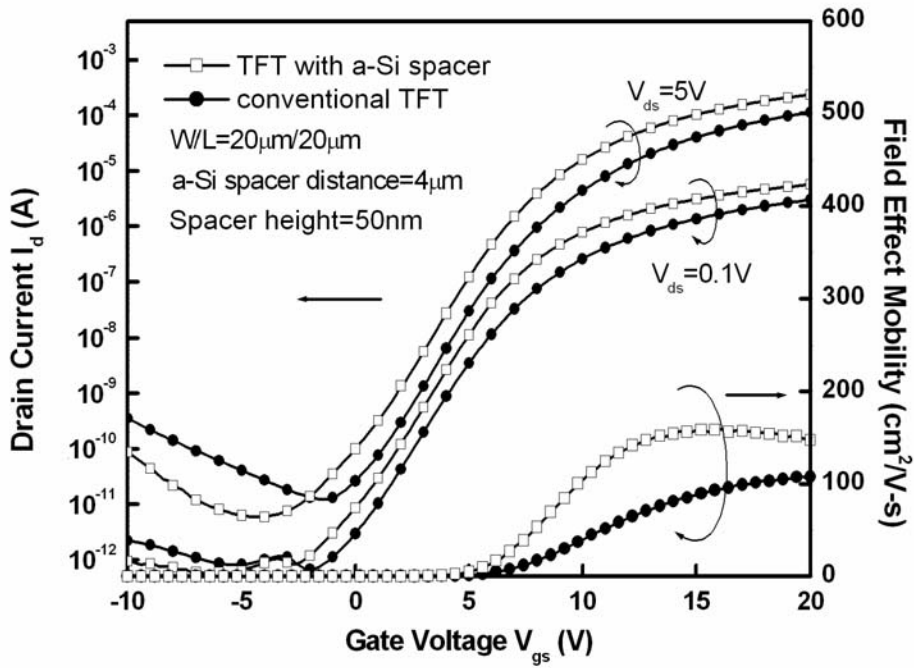


Fig. 4-20(a) Transfer characteristics of ELC poly-Si TFT with 50nm height and 4 μ m distance a-Si spacer structure for W/L=20 μ m/20 μ m and conventional counterpart

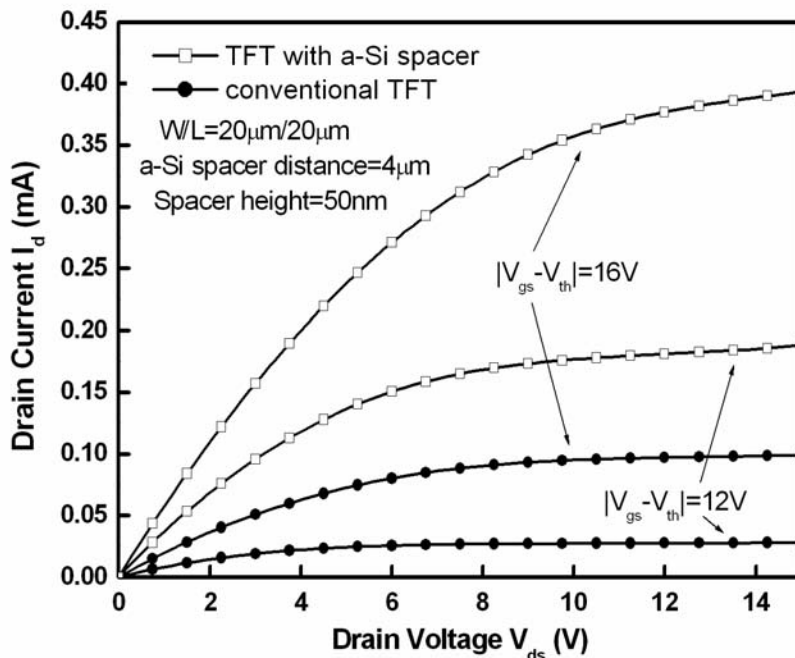


Fig. 4-20(b) Output characteristics of ELC poly-Si TFT with 50nm height and 4 μ m distance a-Si spacer structure for W/L=20 μ m/20 μ m and conventional counterpart

Table 4-4 Electrical characteristics of ELC poly-Si TFT with 50nm height a-Si spacer structure and W/L=10 μ m/10 μ m for different a-Si spacer distance and conventional counterpart

	V_{th} (V)	Mobility (cm ² /V-s)	Sub-threshold Swing (V/dec)	On/Off current ratio
Conventional TFT	6.16	114	1.612	9.27x10 ⁶
Spacer distance = 1μm	5.88	141	1.68	2.49x10 ⁷
Spacer distance = 1.5μm	5.44	147	1.64	2.39x10 ⁷
Spacer distance = 2μm	5.66	167	1.71	1.01x10 ⁷
Spacer distance = 2.5μm	5.68	191	1.52	1.43x10 ⁷
Spacer distance = 3μm	5.49	170	1.61	3.82x10 ⁷
Spacer distance = 4μm	5.64	167	1.67	4.27x10 ⁷

Table 4-5 Electrical characteristics of ELC poly-Si TFT with 50nm height a-Si spacer structure and W/L=20 μ m/20 μ m for different a-Si spacer distance and conventional counterpart

	V_{th} (V)	Mobility (cm ² /V-s)	Sub-threshold Swing (V/dec)	On/Off current ratio
Conventional TFT	5.97	105	1.53	9.26x10 ⁶
Spacer distance = 1μm	5.56	130	1.55	1.10x10 ⁷
Spacer distance = 2μm	4.99	162	1.49	1.95x10 ⁷
Spacer distance = 2.5μm	4.59	176	1.53	1.41x10 ⁷
Spacer distance = 3μm	4.75	159	1.47	3.97x10 ⁷
Spacer distance = 4μm	5.11	151	1.49	2.73x10 ⁷

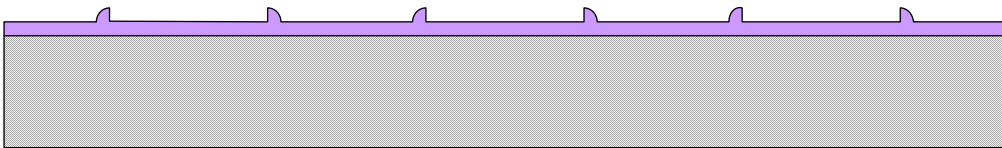
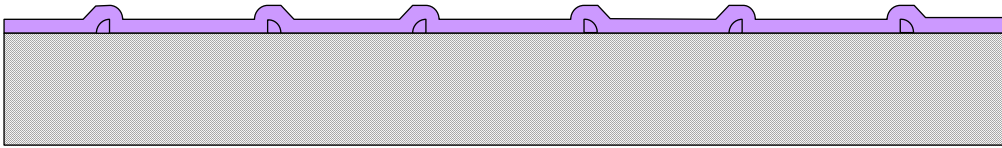


Fig. 5-1 The comparison of two a-Si spacer structures

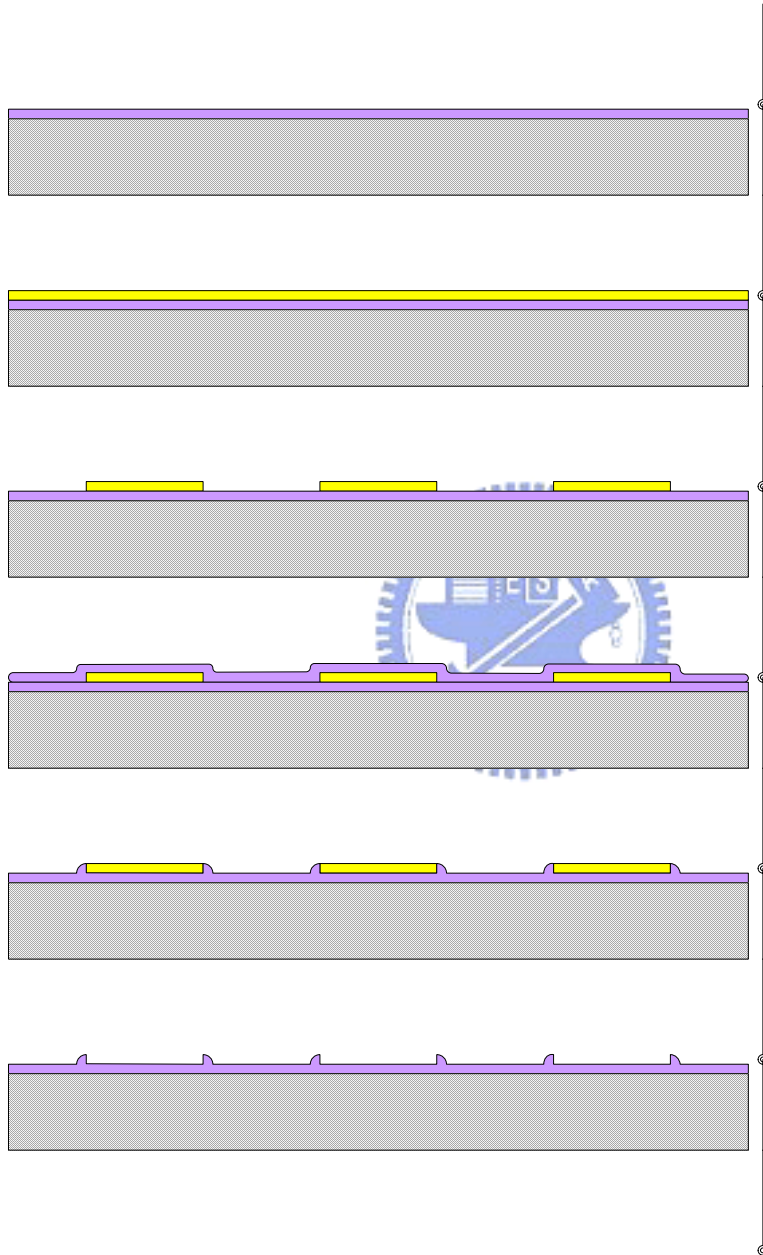
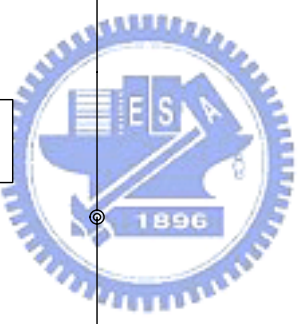
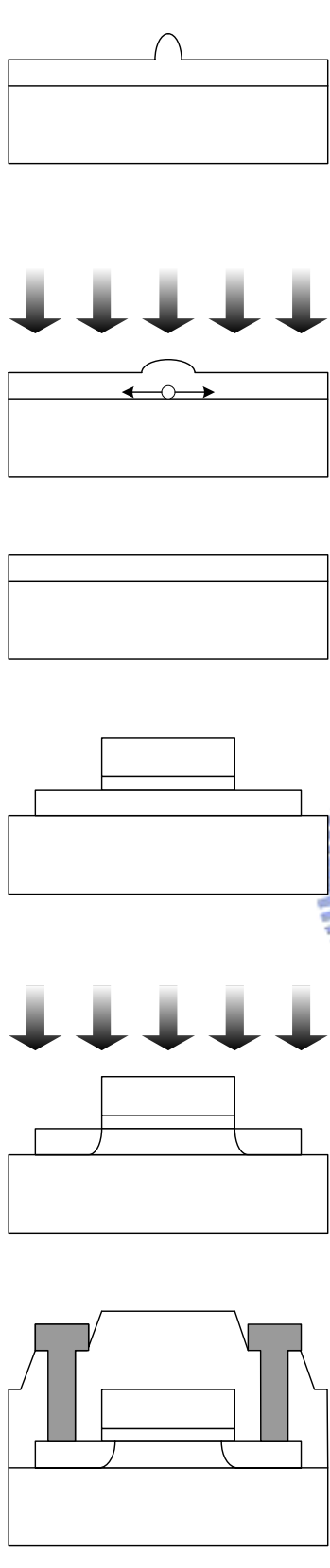


Fig. 5-2 Process flowchart of a-Si spacer structure with pre-patterned TEOS oxide layer



a-Si
 Oxidized Silico
 Excimer Laser I

Fig. 5-3 Process flowchart of ELC LTPS TFT with a-Si spacer structure

Oxidized Silico

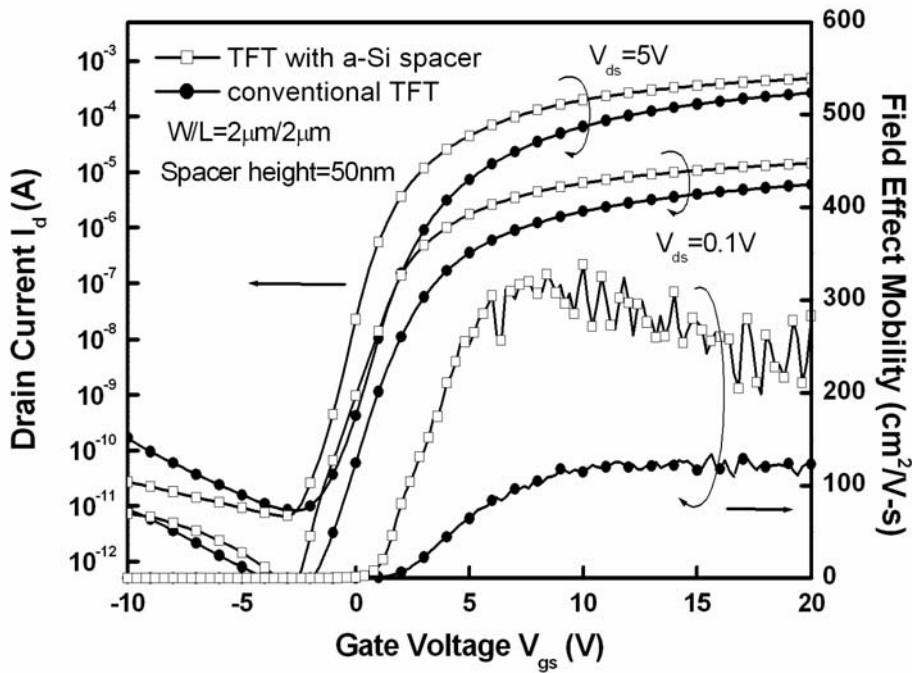


Fig. 5-4(a) Transfer characteristics of ELC LTPS TFT with 50nm height a-Si spacer structure for $W/L=2\mu\text{m}/2\mu\text{m}$ and conventional counterpart

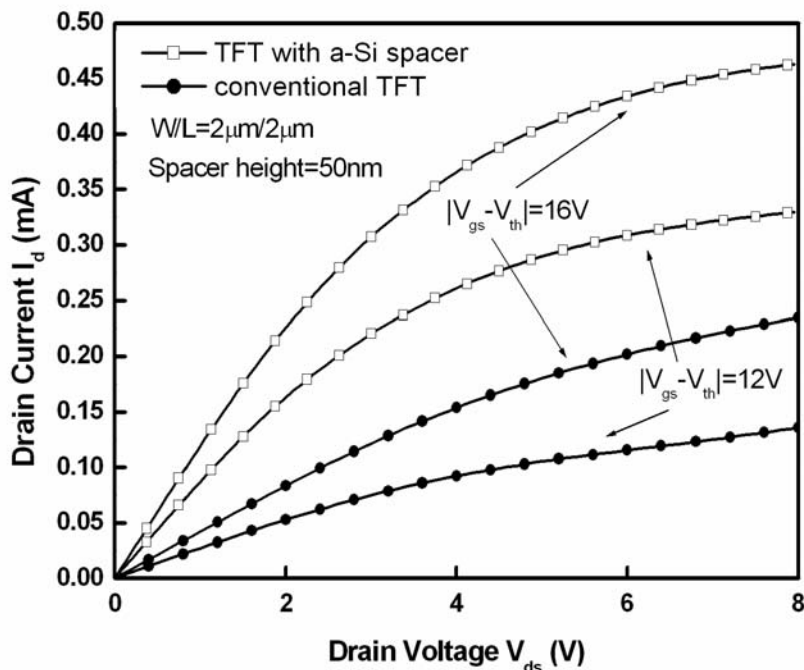


Fig. 5-4(b) Output characteristics of ELC LTPS TFT with 50nm height a-Si spacer structure for $W/L=2\mu\text{m}/2\mu\text{m}$ and conventional counterpart

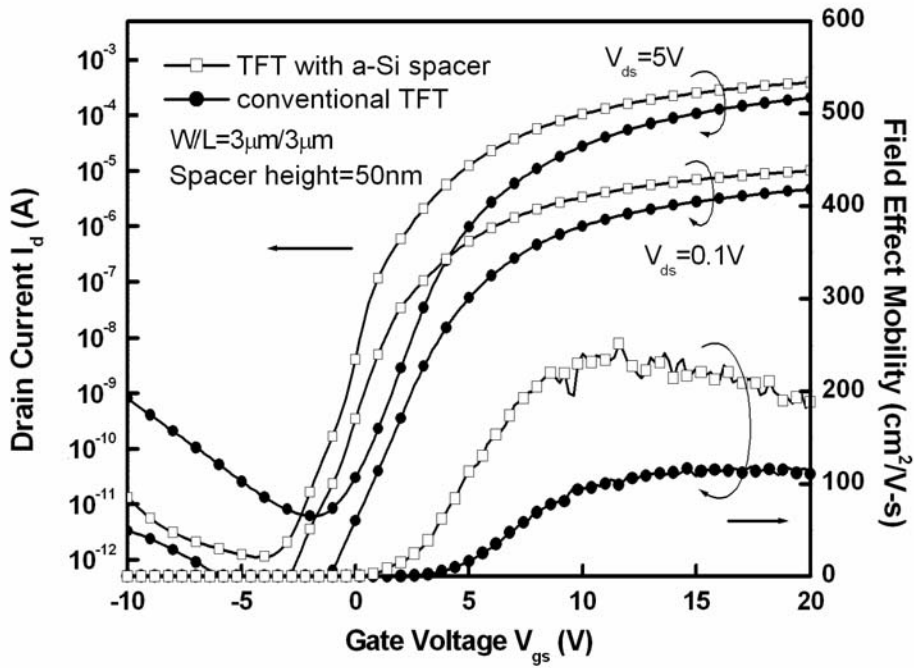


Fig. 5-5(a) Transfer characteristics of ELC LTPS TFT with 50nm height a-Si spacer structure for $W/L=3\mu\text{m}/3\mu\text{m}$ and conventional counterpart

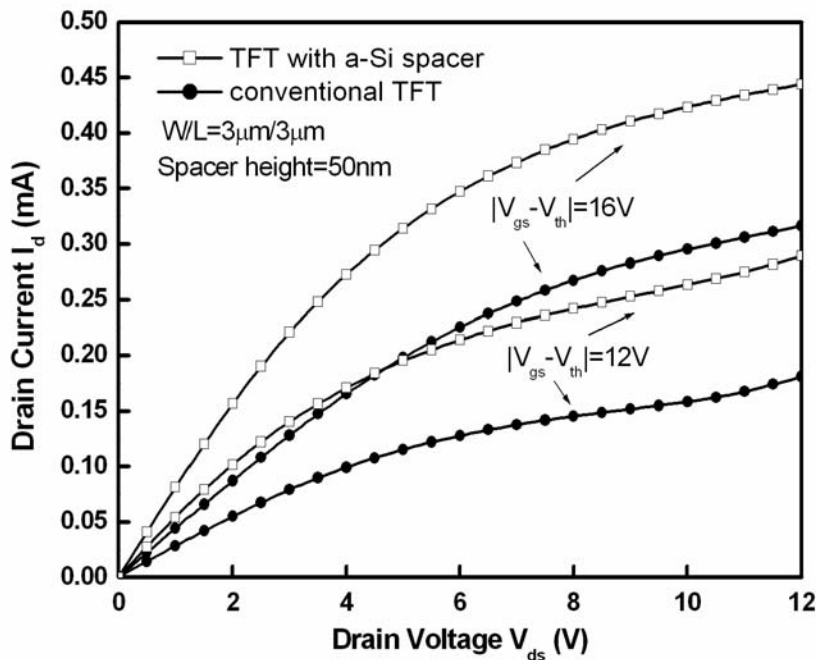


Fig. 5-5(b) Output characteristics of ELC LTPS TFT with 50nm height a-Si spacer structure for $W/L=3\mu\text{m}/3\mu\text{m}$ and conventional counterpart

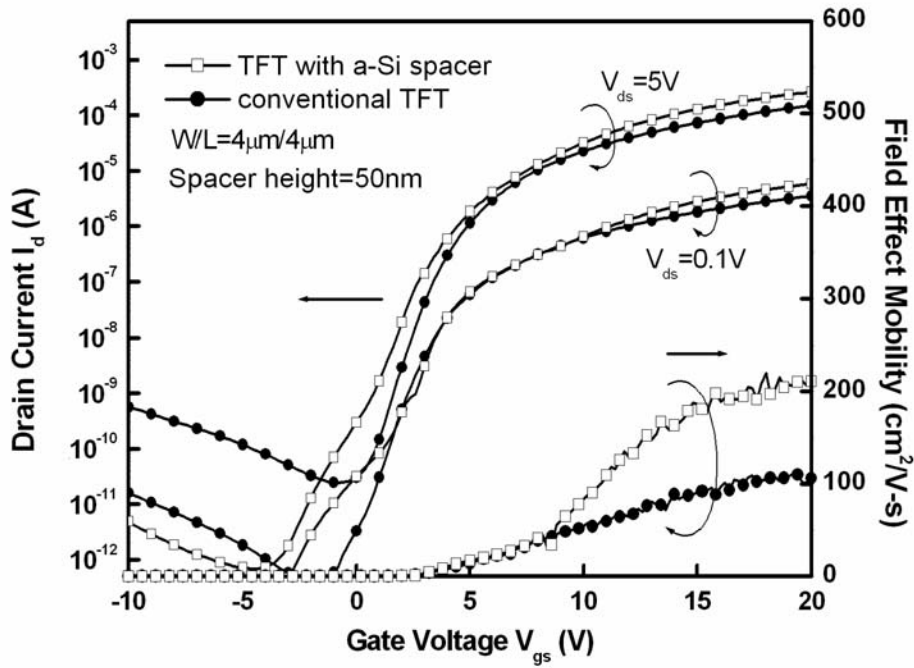


Fig. 5-6(a) Transfer characteristics of ELC LTPS TFT with 50nm height a-Si spacer structure for $W/L=4\mu\text{m}/4\mu\text{m}$ and conventional counterpart

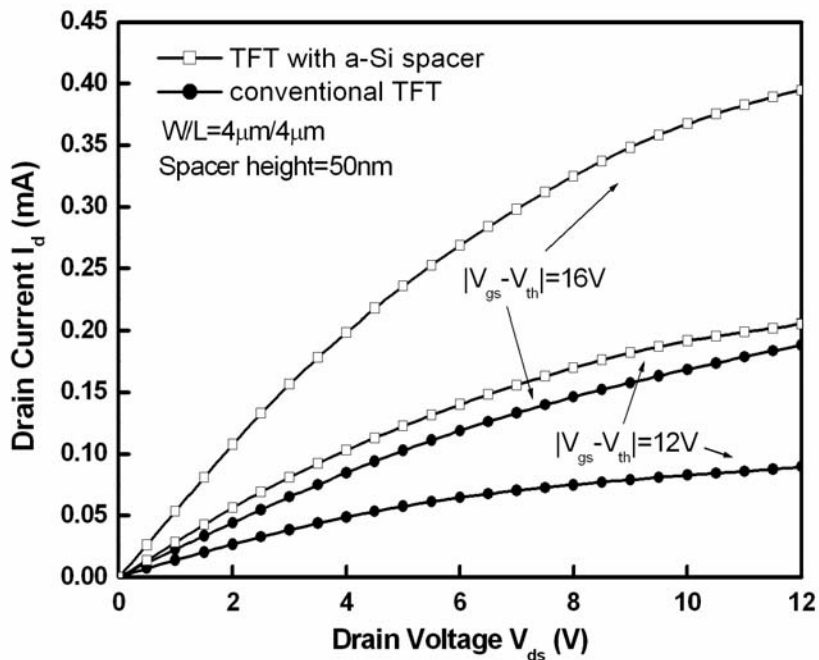


Fig. 5-6(b) Output characteristics of ELC LTPS TFT with 50nm height a-Si spacer structure for $W/L=4\mu\text{m}/4\mu\text{m}$ and conventional counterpart

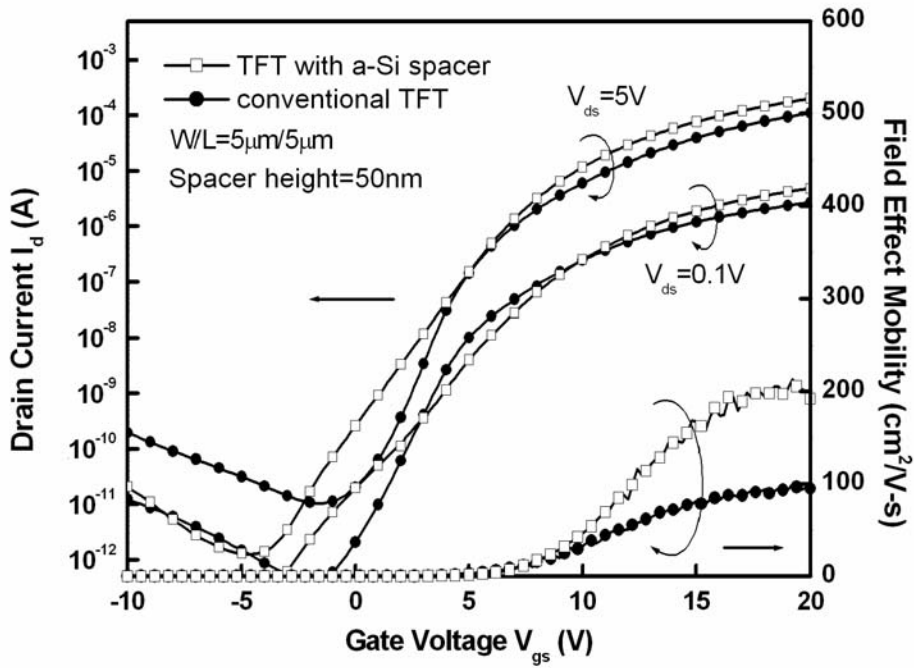


Fig. 5-7(a) Transfer characteristics of ELC LTPS TFT with 50nm height a-Si spacer structure for $W/L=5\mu\text{m}/5\mu\text{m}$ and conventional counterpart

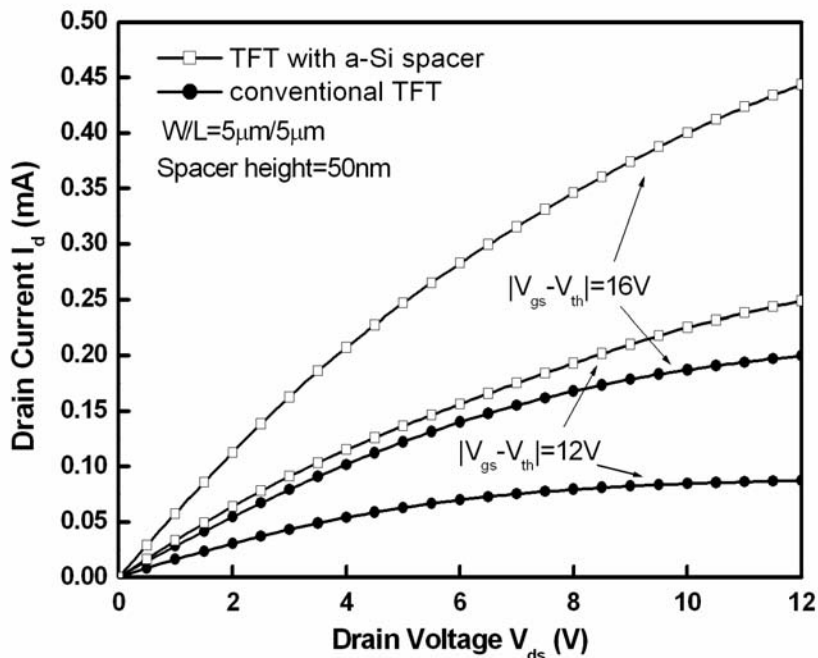


Fig. 5-7(b) Output characteristics of ELC LTPS TFT with 50nm height a-Si spacer structure for $W/L=5\mu\text{m}/5\mu\text{m}$ and conventional counterpart

Table 5-1 Electrical characteristics of ELC LTPS TFT with 50nm height a-Si spacer structure for different device dimension and conventional counterpart

	V_{th} (V)	Mobility (cm ² /V-s)	Sub-threshold Swing (mV/dec)	On/Off current ratio
Conventional TFT (W=L=2um)	1.94	128	738	3.32x10 ⁷
TFT with Si spacer (W=L=2um)	-0.232	367	477	6.31x10⁷
Conventional TFT (W=L=3um)	3.72	116	1010	3.41x10 ⁷
TFT with Si spacer (W=L=3um)	1.324	251	743	3.52x10⁸
Conventional TFT (W=L=4um)	3.44	108	779	6.23x10 ⁶
TFT with Si spacer (W=L=4um)	3.491	220	785	3.89x10⁸
Conventional TFT (W=L=5um)	4.99	97	1170	1.04x10 ⁷
TFT with Si spacer (W=L=5um)	5.908	213	1691	1.6x10⁸

Table 5-2 Electrical characteristics of ELC poly-Si TFT with 50nm height a-Si spacer structure for different pre-patterned layer and device dimension

	V_{th} (V)	Mobility (cm ² /V-s)	Sub-threshold Swing (mV/dec)	On/Off current ratio
TEOS oxide (W=L=2um)	-0.232	367	477	6.31x10⁷
Nitride (W=L=2um)	0.976	289	672	3.68x10 ⁷
TEOS oxide (W=L=3um)	1.324	251	743	3.52x10⁸
Nitride (W=L=3um)	3.53	206	944	6.81x10 ⁷
TEOS oxide (W=L=4um)	3.491	220	785	3.89x10⁸
Nitride (W=L=4um)	2.29	198	704	5.73x10 ⁷
TEOS oxide (W=L=5um)	5.908	213	1691	1.6x10⁸
Nitride (W=L=5um)	4.84	169	1170	3.6x10 ⁷

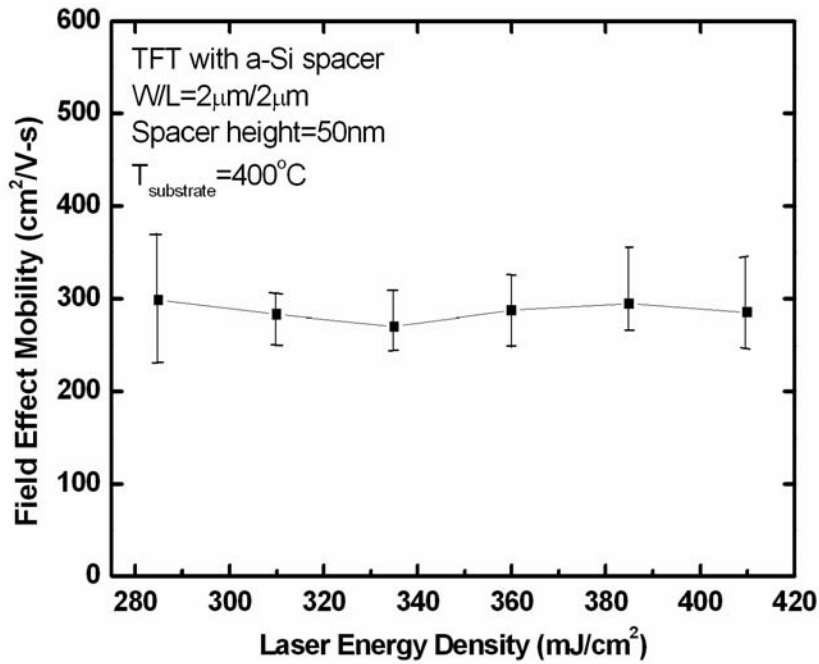


Fig. 5-8(a) Dependence of field effect mobility on laser energy density of ELC LTPS TFT with 50nm height a-Si spacer structure for $W/L=2\mu\text{m}/2\mu\text{m}$ and substrate heating to 400°C

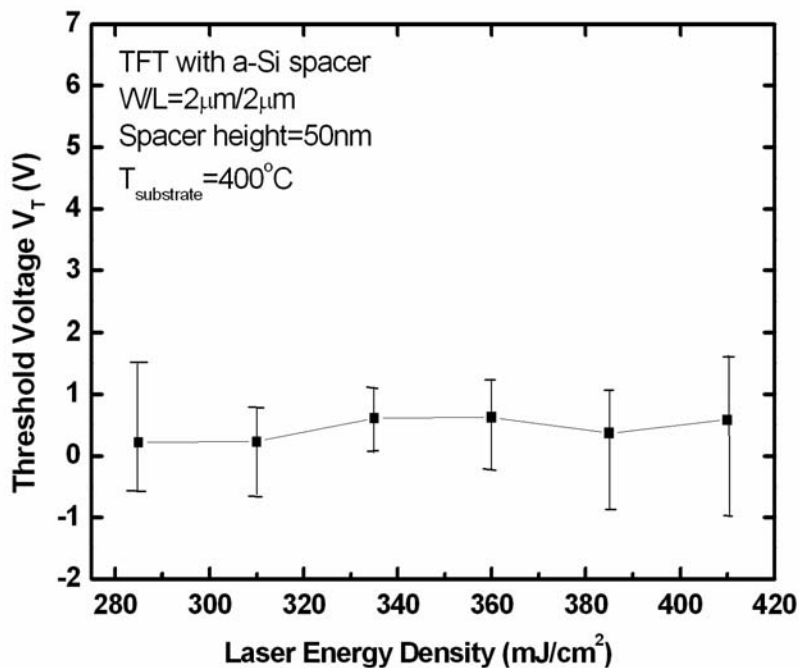


Fig. 5-8(b) Dependence of threshold voltage on laser energy density of ELC LTPS TFT with 50nm height a-Si spacer structure for $W/L=2\mu\text{m}/2\mu\text{m}$ and substrate heating to 400°C

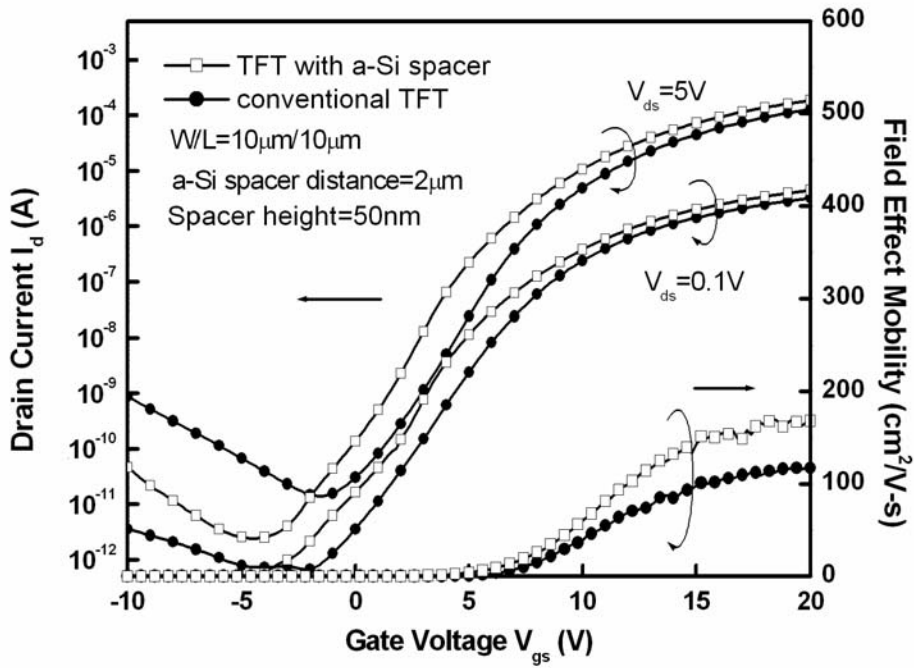


Fig. 5-9(a) Transfer characteristics of ELC LTPS TFT with 50nm height and $2\mu\text{m}$ distance a-Si spacer structure for $W/L=10\mu\text{m}/10\mu\text{m}$ and conventional counterpart

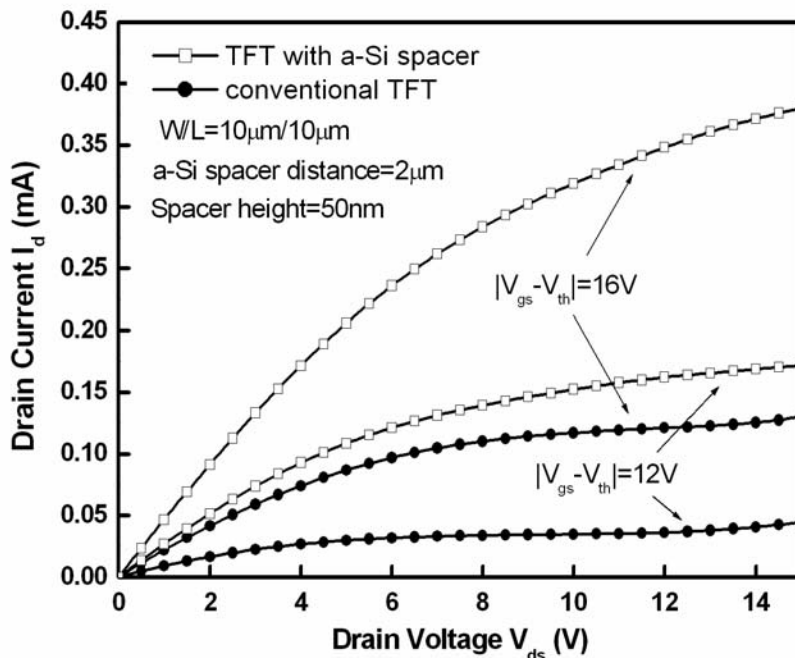


Fig. 5-9(b) Output characteristics of ELC LTPS TFT with 50nm height and $2\mu\text{m}$ distance a-Si spacer structure for $W/L=10\mu\text{m}/10\mu\text{m}$ and conventional counterpart

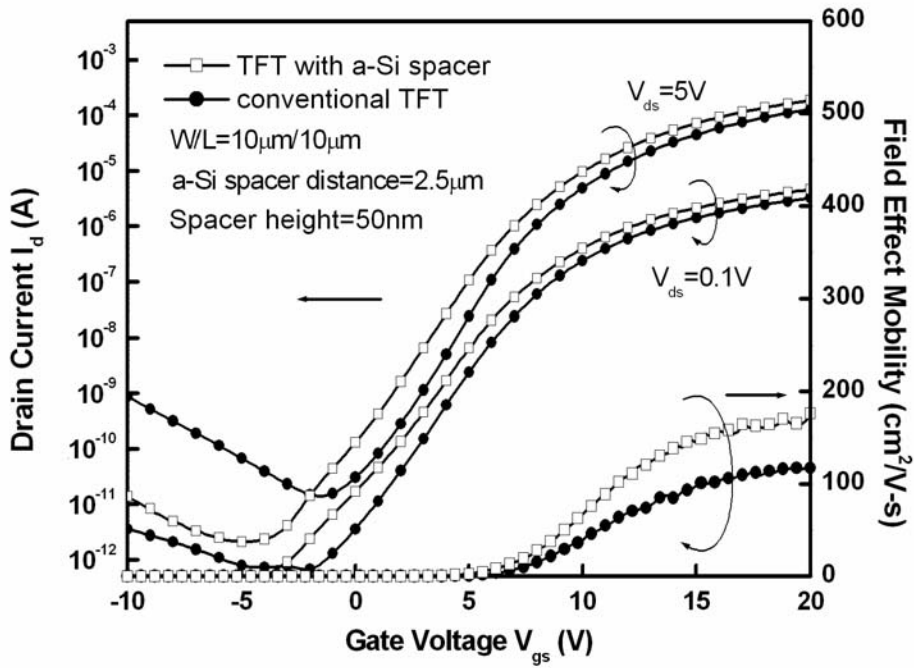


Fig. 5-10(a) Transfer characteristics of ELC LTPS TFT with 50nm height and 2.5 μ m distance a-Si spacer structure for W/L=10 μ m/10 μ m and conventional counterpart

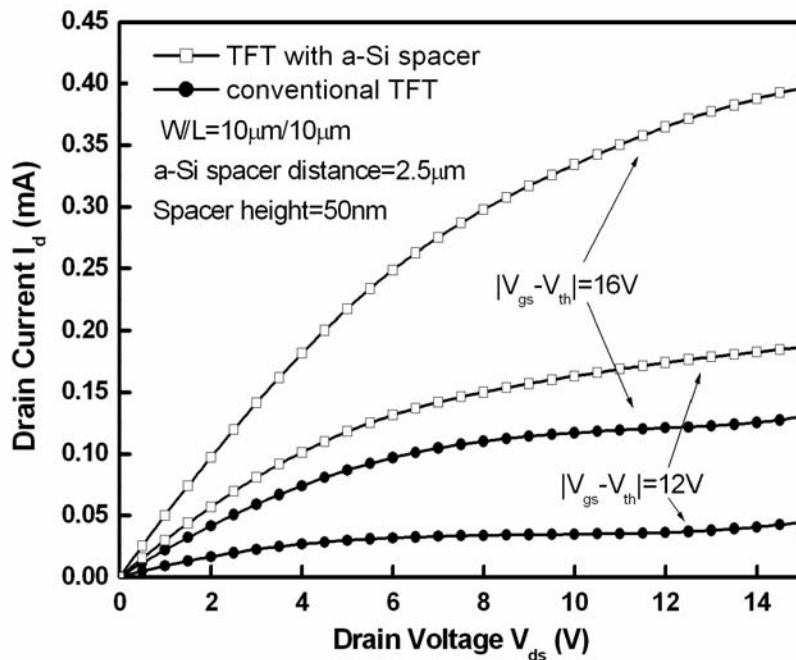


Fig. 5-10(b) Output characteristics of ELC LTPS TFT with 50nm height and 2.5 μ m distance a-Si spacer structure for W/L=10 μ m/10 μ m and conventional counterpart

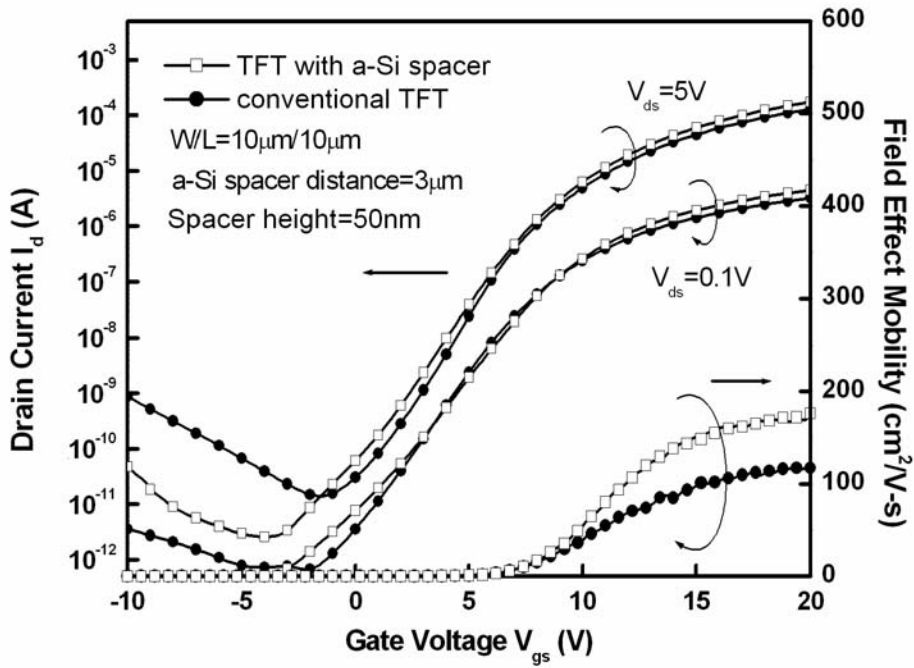


Fig. 5-11(a) Transfer characteristics of ELC LTPS TFT with 50nm height and 3 μ m distance a-Si spacer structure for W/L=10 μ m/10 μ m and conventional counterpart

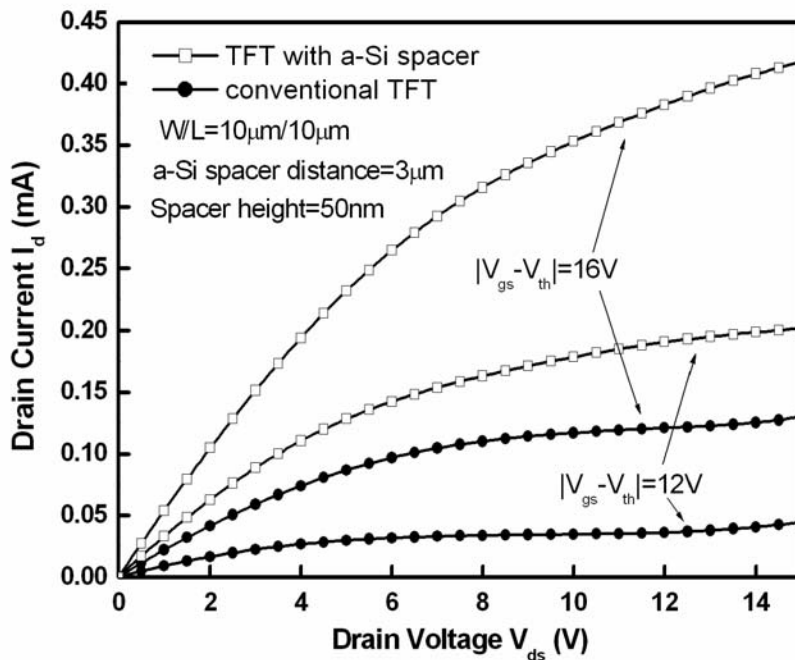


Fig. 5-11(b) Output characteristics of ELC LTPS TFT with 50nm height and 3 μ m distance a-Si spacer structure for W/L=10 μ m/10 μ m and conventional counterpart

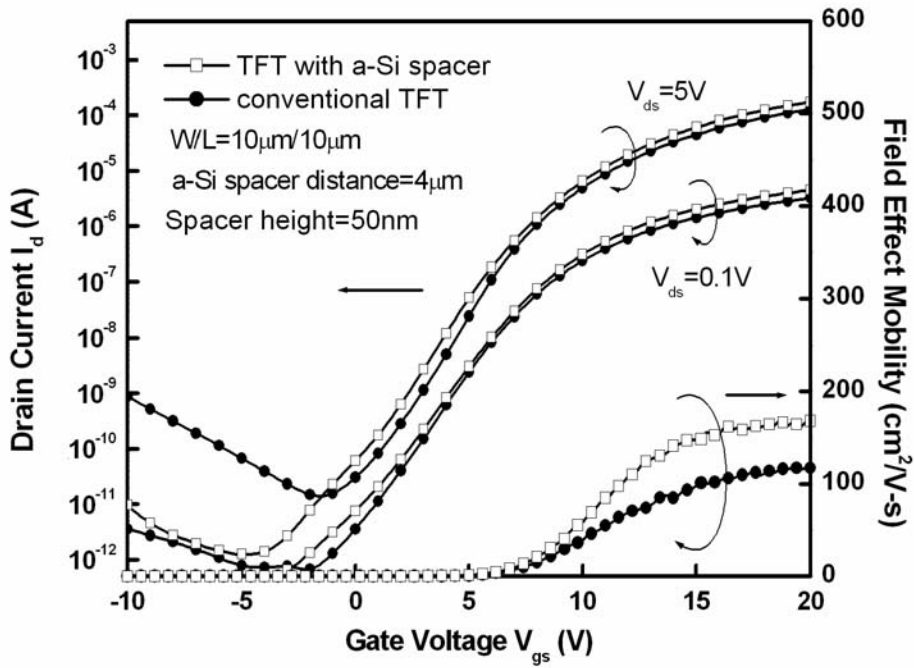


Fig. 5-12(a) Transfer characteristics of ELC LTPS TFT with 50nm height and 4 μ m distance a-Si spacer structure for W/L=10 μ m/10 μ m and conventional counterpart

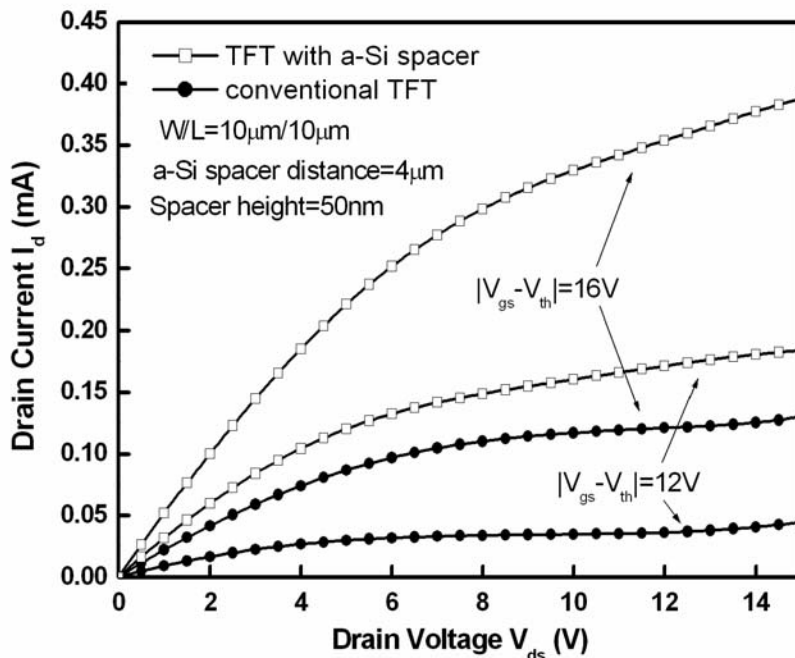


Fig. 5-12(b) Output characteristics of ELC LTPS TFT with 50nm height and 4 μ m distance a-Si spacer structure for W/L=10 μ m/10 μ m and conventional counterpart

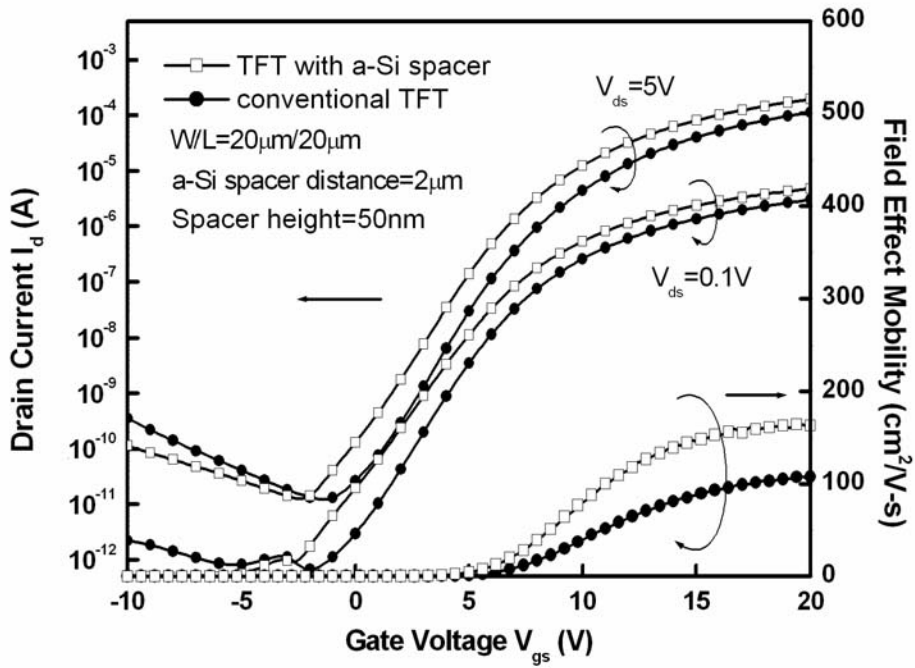


Fig. 5-13(a) Transfer characteristics of ELC LTPS TFT with 50nm height and 2 μ m distance a-Si spacer structure for W/L=20 μ m/20 μ m and conventional counterpart

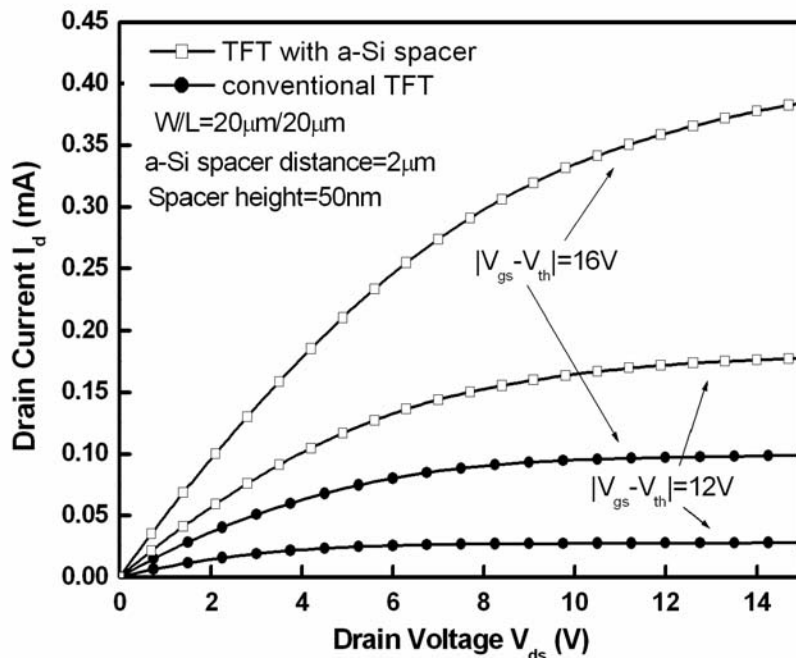


Fig. 5-13(b) Output characteristics of ELC LTPS TFT with 50nm height and 2 μ m distance a-Si spacer structure for W/L=20 μ m/20 μ m and conventional counterpart

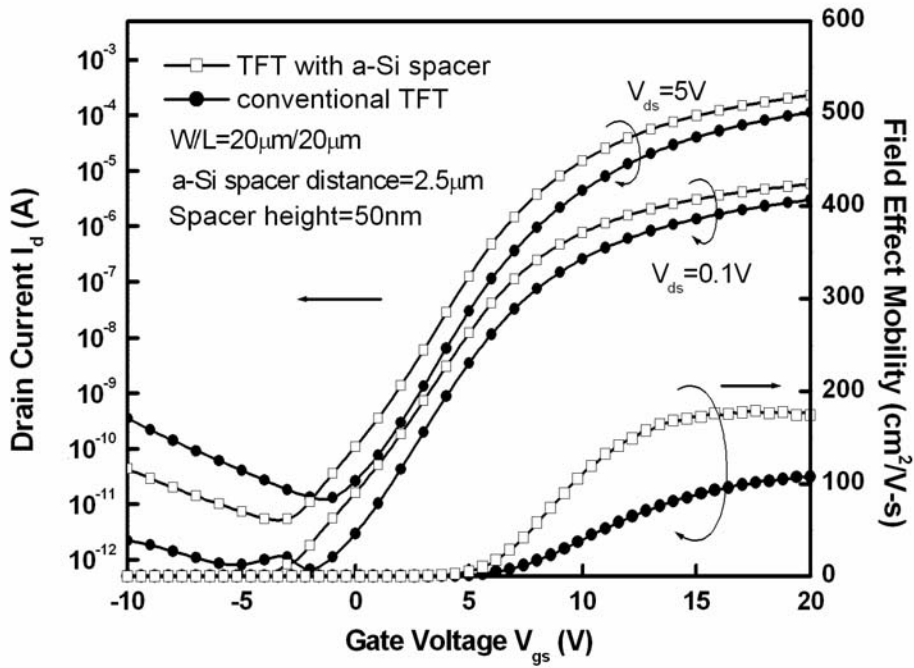


Fig. 5-14(a) Transfer characteristics of ELC LTPS TFT with 50nm height and 2.5 μ m distance a-Si spacer structure for W/L=20 μ m/20 μ m and conventional counterpart

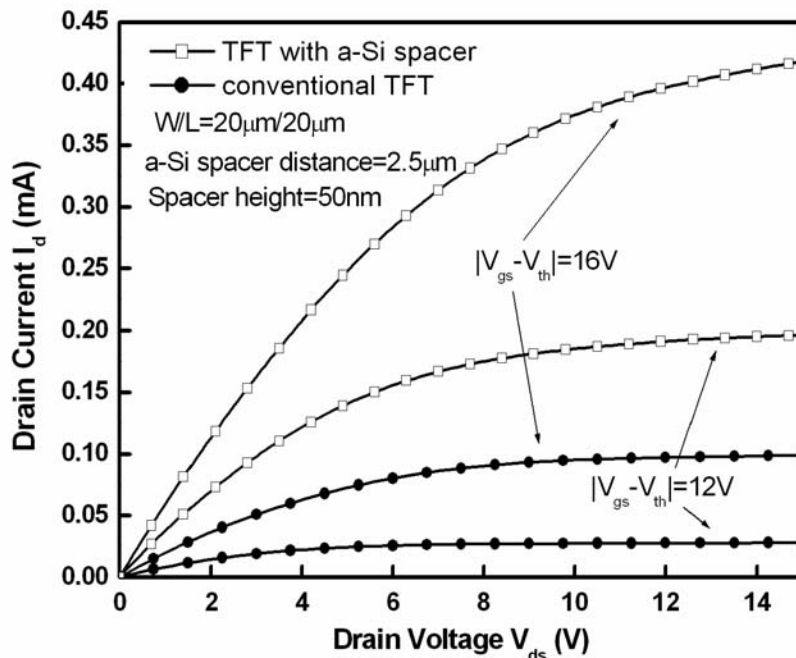


Fig. 5-14(b) Output characteristics of ELC LTPS TFT with 50nm height and 2.5 μ m distance a-Si spacer structure for W/L=20 μ m/20 μ m and conventional counterpart

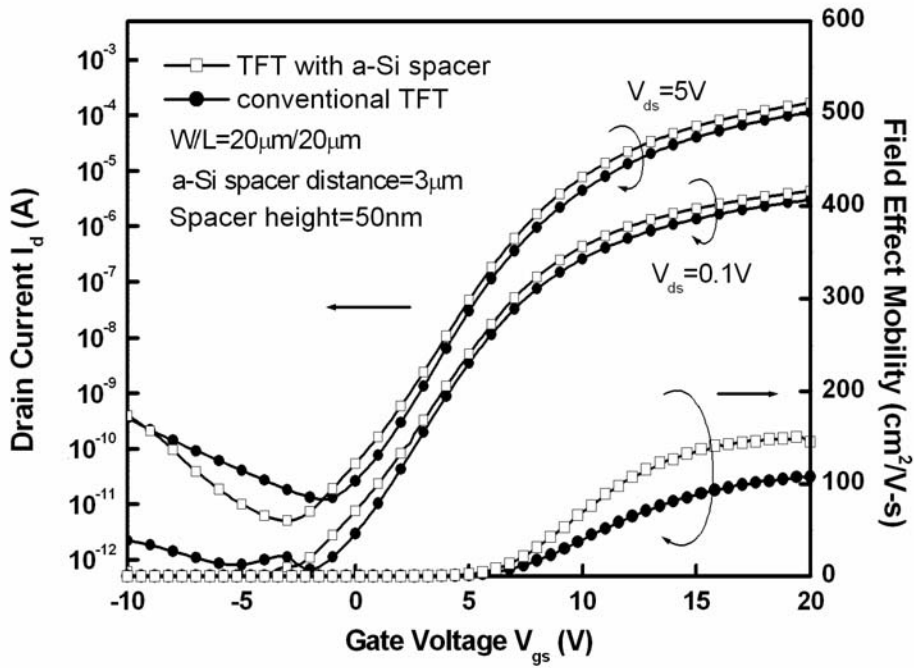


Fig. 5-15(a) Transfer characteristics of ELC LTPS TFT with 50nm height and 3 μ m distance a-Si spacer structure for W/L=20 μ m/20 μ m and conventional counterpart

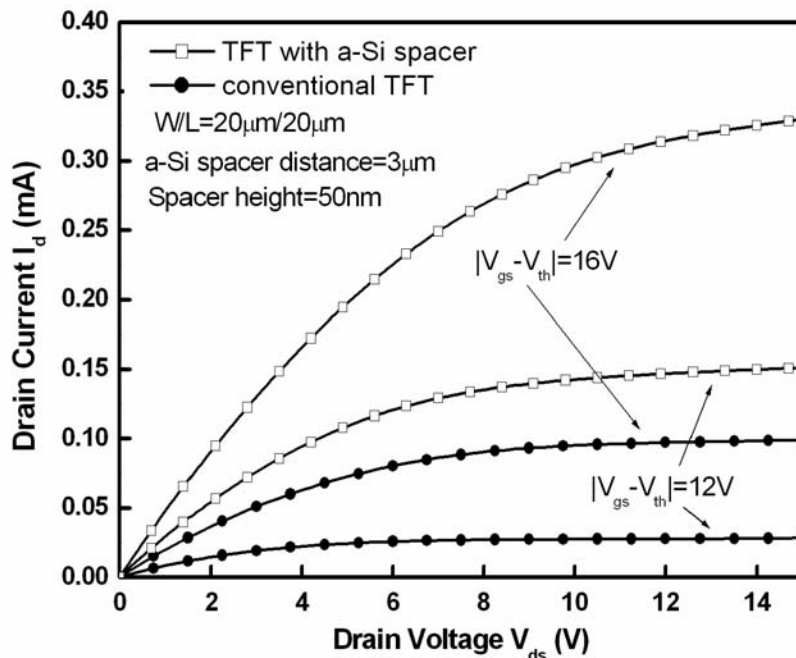


Fig. 5-15(b) Output characteristics of ELC LTPS TFT with 50nm height and 3 μ m distance a-Si spacer structure for W/L=20 μ m/20 μ m and conventional counterpart

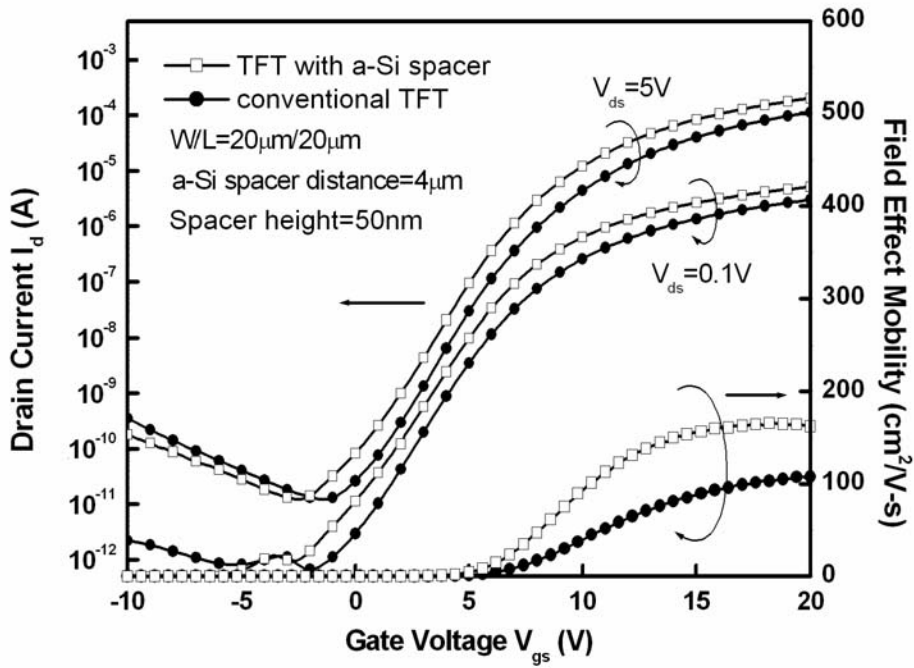


Fig. 5-16(a) Transfer characteristics of ELC LTPS TFT with 50nm height and $4\mu\text{m}$ distance a-Si spacer structure for $W/L=20\mu\text{m}/20\mu\text{m}$ and conventional counterpart

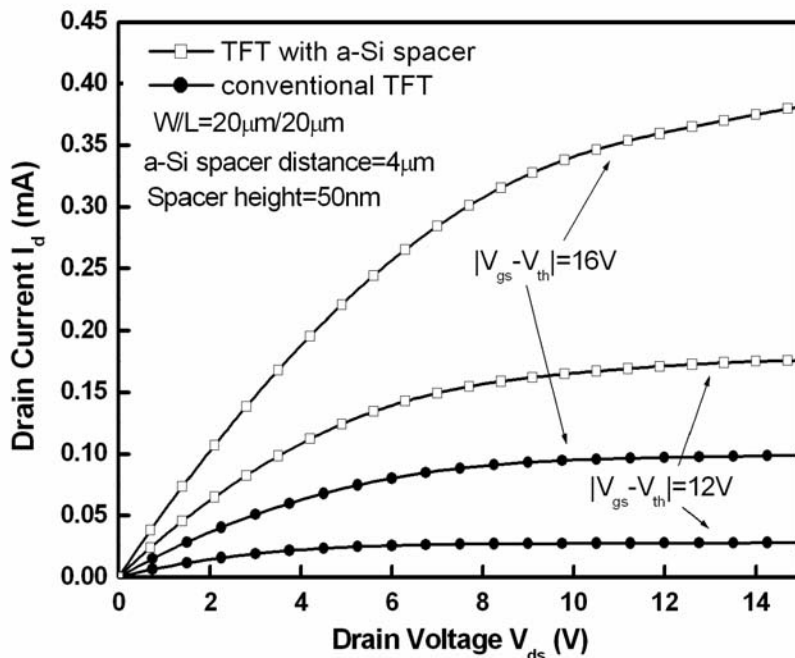


Fig. 5-16(b) Output characteristics of ELC LTPS TFT with 50nm height and $4\mu\text{m}$ distance a-Si spacer structure for $W/L=20\mu\text{m}/20\mu\text{m}$ and conventional counterpart

Table 5-3 Electrical characteristics of ELC LTPS TFT with 50nm height a-Si spacer structure and W/L=10 μ m/10 μ m for different a-Si spacer distance and conventional counterpart

	V_{th} (V)	Mobility (cm ² /V-s)	Sub-threshold Swing (V/dec)	On/Off current ratio
Conventional TFT	6.16	114	1.612	9.27x10 ⁶
Spacer distance = 2μm	4.883	170	1.274	7.76x10⁷
Spacer distance = 2.5μm	5.353	176	1.604	8.92x10⁷
Spacer distance = 3μm	6.403	176	1.806	6.81x10⁷
Spacer distance = 4μm	5.995	168	1.735	1.4x10⁸



Table 5-4 Electrical characteristics of ELC LTPS TFT with 50nm height a-Si spacer structure and W/L=20 μ m/20 μ m for different a-Si spacer distance and conventional counterpart

	V_{th} (V)	Mobility (cm ² /V-s)	Sub-threshold Swing (V/dec)	On/Off current ratio
Conventional TFT	5.97	105	1.53	9.26x10 ⁶
Spacer distance = 2μm	4.902	164	1.72	1.56x10 ⁷
Spacer distance = 2.5μm	4.86	179	1.614	4.44x10 ⁷
Spacer distance = 3μm	5.542	151	1.377	3.26x10 ⁷
Spacer distance = 4μm	4.819	166	1.354	2.51x10 ⁷